Phosphate-binding pocket on cyclin B governs CDK substrate phosphorylation and mitotic timing

Henry Y. Ng[1], Armin N. Adly[1], Devon H. Whelpley[1], Raymond T. Suhandynata[2,3], Huilin Zhou[4], David O. Morgan[1*]

[1]Department of Physiology, University of California San Francisco, San Francisco CA

[2]School of Pharmacy and Pharmaceutical Sciences, University of California San Diego, La Jolla CA

[3]Department of Pathology, University of California San Diego, La Jolla CA

[4]Department of Cellular and Molecular Medicine, University of California San Diego, La Jolla CA

[*]Correspondence: David.morgan@ucsf.edu

Summary

Cell cycle progression is governed by complexes of the cyclin-dependent kinases (CDKs) and their regulatory subunits cyclin and Cks1. CDKs phosphorylate hundreds of substrates, often at multiple sites. Multisite phosphorylation depends on Cks1, which binds initial priming phosphorylation sites to promote secondary phosphorylation at other sites. Here, we describe a similar role for a recently discovered phosphate-binding pocket (PP) on B-type cyclins. Mutation of the PP in Clb2, the major mitotic cyclin of budding yeast, alters bud morphology and delays the onset of anaphase. Using phosphoproteomics *in vivo* and kinase reactions *in vitro*, we find that mutation of the PP reduces phosphorylation of several CDK substrates, including the Bud6 subunit of the polarisome and the Cdc16 and Cdc27 subunits of the anaphase-promoting complex/cyclosome. We conclude that the cyclin PP, like Cks1, controls the timing of multisite phosphorylation on CDK substrates, thereby helping to establish the robust timing of cell-cycle events.

Introduction

Complexes of cyclin-dependent kinases (CDKs) and their cyclin regulatory subunits phosphorylate hundreds of protein substrates to drive progression through the phases of the cell division cycle[1–5]. Phosphorylation generally occurs at serines or threonines followed by a proline, sometimes followed by a basic residue to form the optimal consensus site, S/T*-P-x-K/R. Multiple CDK sites are often clustered in long regions of intrinsic disorder[2]. Multisite phosphorylation in these regions alters the activity, binding partners, localization, or turnover of the regulatory and structural proteins that drive cell cycle events[6–9].

CDK substrates are phosphorylated at specific times during the cell cycle, ensuring the correct sequence and coordination of cell cycle events. The timing of substrate phosphorylation

depends on many mechanisms. Due to variations in sequence context and accessibility, different CDK phosphorylation sites exhibit wide variations in their rates of phosphorylation[1–5], likely resulting in differences in the timing of phosphorylation. Many substrates carry short linear sequence motifs (SLiMs) that interact with docking sites on a specific cyclin regulatory subunit, thereby promoting phosphorylation at cell cycle stages when that cyclin is expressed[3,10,11]. For example, an L-x-F motif on some substrates docks at a site called the hydrophobic patch of cyclin B[11]. The timing of substrate phosphorylation is also determined, at least in part, by the level of CDK activity, such that certain substrates are modified earlier in the cycle at low CDK activity and other substrates are modified later by rising levels of activity[4,5,7,8,12,13]. Phosphatase specificity for different sites is also likely to contribute to the timing of phosphorylation[14–19].

Some CDK–substrate interactions are influenced by the small accessory protein Cks1, which binds to the CDK subunit of the cyclin-CDK complex[8,13,20–25]. Cks1 has a phosphate-binding pocket with specificity for phosphorylated threonine. After initial phosphorylation of a CDK substrate at a threonine, Cks1 binds to the phosphothreonine to promote secondary phosphorylation of the substrate at downstream serines or threonines, leading to sequential multisite phosphorylation[13,24,25]. Cks1 is required for multisite phosphorylation of numerous CDK substrates. In the case of the CDK inhibitor Sic1, Cks1 promotes secondary phosphorylation at 'phosphodegron' motifs that trigger Sic1 ubiquitylation and destruction[8]. Cks1-dependent secondary site phosphorylation is thought to provide a mechanism to delay cell cycle events until CDK activity reaches a higher threshold.

Recent structural studies revealed that human cyclin B1 carries a binding pocket for a phosphorylation site in the CDK substrate, separase[23]. This phospho-pocket (PP) is formed by the positively charged side chains of three amino acids, R307, H320 and K324, on the surface of cyclin B1 near the Cdk1 active site. These residues are highly conserved in B-type cyclins

(Figure 1A, S1A), supporting a conserved role for phosphate binding at this site. The discovery of this phosphate-binding site raised the possibility that B-type cyclins, like Cks1, interact with phosphorylation sites on Cdk1 substrates to promote secondary phosphorylation at other sites.

We showed recently that mutation of the PP in budding yeast Clb2 reduces phosphorylation of Ndd1, a transcriptional co-activator that stimulates *CLB2* expression in early mitosis[7]. Ndd1 has 16 consensus CDK phosphorylation sites. Initial phosphorylation of one site, T319, promotes Ndd1 function and *CLB2* expression in early mitosis, resulting in positive feedback[26]. When CDK activity reaches high levels in mitosis, hyperphosphorylation of Ndd1 at multiple additional sites promotes its degradation, thereby suppressing *CLB2* expression. *In vitro*, large numbers of sites in Ndd1 are phosphorylated by wild-type Clb2-Cdk1-Cks1 complexes. Mutation of either Cks1 or the Clb2 PP does not affect initial phosphorylation sites but reduces phosphorylation at later sites, suggesting that the cyclin PP, together with Cks1, is required for secondary phosphorylation at sites that promote Ndd1 degradation.

In budding yeast, four B-type cyclins (Clb1-4) contribute to the control of mitosis. Clb2 is the major mitotic cyclin, working with Cdk1 to catalyze phosphorylation of numerous proteins involved in mitotic processes, including spindle assembly, bud growth, and bud morphology[27–29]. It is also involved in the phosphorylation, and thus activation, of the Anaphase-Promoting Complex/Cyclosome (APC/C), the ubiquitin ligase responsible for triggering chromosome segregation in anaphase[30,31]. Deletion of *CLB2* is not lethal but causes elongated bud morphology and mitotic delays. *CLB2* is essential for survival in the absence of *CLB1* and *CLB3*[29], revealing that mitotic progression depends on contributions from multiple cyclins.

As multisite phosphorylation of CDK substrates plays an important role in cell cycle regulation, we asked whether mutation of the PP in Clb2 leads to cell cycle defects. Our results suggest

that mutation of the PP causes a delay in mitotic timing, particularly when combined with deletions of *CLB1* and *CLB3*. We find that the multisite phosphorylation of several Cdk1 substrates, including subunits of the APC/C, is reduced *in vitro* by mutation of the Clb2 PP. We conclude that the precise timing of mitotic events depends in part on PP-dependent multisite phosphorylation of CDK substrates in the cell.

Results

The Clb2 phosphate pocket is required for normal cell proliferation

To characterize the functions and biochemical properties of the phosphate pocket in B-type cyclins, we analyzed the role of the pocket in the budding yeast *Saccharomyces cerevisiae*. The three basic residues that constitute the phosphate-binding pocket of human cyclin B1 are highly conserved not only among paralogs but also orthologs from different species (Figure 1A, S1A). Due to its high conservation, we hypothesized that the phosphate-binding pocket plays an important role in B-type cyclin function.

Four B-type cyclins (Clb1-4) are involved in the control of mitosis in budding yeast. Clb2 is the major mitotic regulator, and we therefore focused our studies on the phosphate pocket of Clb2. As described in our previous work, we constructed a strain in which *CLB2* is replaced by a mutant allele in which the three key pocket residues are mutated to alanine – termed the *clb2-pp* mutant (R366A, R379A, K383A)[7].

Mutation of the Clb2 phosphate pocket did not cause apparent proliferation defects at 30°C on rich media (Figure S1B). To examine whether other B-type cyclins compensate for the loss of the Clb2 PP, we introduced single or multiple deletion mutations in a *clb2-pp* background. In previous work, combinations of *CLB* deletions with *clb2*Δ (*i.e. clb1*Δ *clb2*Δ*, clb2*Δ *clb3*Δ*, clb1*Δ

*clb2*Δ *clb3*Δ*, clb1*Δ *clb2*Δ *clb4*Δ*,* and *clb1*Δ *clb2*Δ *clb3*Δ *clb4*Δ) caused severe growth defects or lethality[29,32]. We found, however, that combining deletions with *clb2-pp* resulted in viable colonies (*clb1*Δ *clb2-pp, clb2-pp clb3*Δ*, clb1*Δ *clb2-pp clb3*Δ) (Figure S1B).

To provide a more detailed understanding of cell proliferation, we measured growth rate in suspension cultures using an optical density-based method (Figure 1B). At 30°C in rich media, all single and double mutants grew at rates that were not significantly different from that of the wild-type strain. A defect was seen only in the triple mutant, *clb1*Δ *clb2-pp clb3*Δ, which grew at a rate about 40% lower than that of the wild-type (Figure 1B). Thus, in the absence of *CLB1* and *CLB3, clb2-pp* is not sufficient for normal rates of proliferation.

To further examine the role of the Clb2 PP, we sensitized the strains with heat stress or microtubule destabilization. The *clb1*Δ *clb3*Δ *and clb1*Δ *clb2-pp clb3*Δ mutants showed a mild growth defect at 37°C (Figure S1B, middle). Any double or triple mutant showed a mild growth defect when treated with a low concentration of benomyl, a microtubule destabilizer (Figure S1B, right).

Analysis by microscopy revealed that cells of the *clb2-pp* strain do not display an elongated morphology phenotype like that seen in a *clb2*Δ strain[29,32] (Figure 1C). *clb2-pp clb3*Δ cells showed a mild elongated morphology, while *clb1*Δ *clb2-pp and clb1*Δ *clb2-pp clb3*Δ cells displayed a more pronounced elongated phenotype accompanied by cell chains (Figure 1C). Thus, the phosphate pocket is required for the normal function of Clb2 in bud morphology.

The Clb2 phosphate pocket is required for normal mitotic progression

We next investigated the role of the Clb2 PP in progression through mitosis. As in our previous work, we measured mitotic progression in single cells by analyzing the behavior of a fluorescently tagged spindle pole body (SPB)[33]. The SPB is duplicated in early S phase and separates slightly at the onset of mitosis to form the short mitotic spindle; the initiation of anaphase then triggers rapid SPB separation as the spindle elongates across the mother cell and into the bud[34,35]. The time between initial SPB separation and spindle elongation reflects the time from mitotic entry to anaphase onset.

We constructed wild-type and *clb2-pp* strains in which the SPB protein Spc42 was fused to a C-terminal mCherry fluorophore, and we measured the time from SPB separation to spindle elongation (Figure 2A, S2A). As in our previous studies, this time was highly variable in wild-type cells, ranging from 10 to 66 min with a median of 32 min[33]. In comparison, *clb2-pp* mutant cells displayed a range of 20 to 82 min, with a median of 48 min. Thus, *clb2-pp* cells experience a ~15-minute delay in a ~30-minute process (Figure 2A). We conclude that the Clb2 PP is required for the normal timing of progression through mitosis to anaphase onset.

We next analyzed mitotic progression by western blotting of mitotic proteins in cells released from a G1 arrest. We first analyzed the separase inhibitor securin/Pds1, which is known to increase in abundance in S phase and then decline rapidly at the onset of anaphase due to its ubiquitination by the Cdc20-activated APC/C. Mutation of the Clb2 PP resulted in a small but reproducible delay in the timing of securin destruction (Figure 2B, left). Deletion of *CLB1* and *CLB3* had no significant impact on securin degradation, but *clb1*Δ *clb2-pp clb3*Δ cells showed a major delay in securin degradation past 120 min after release from G1 (Figure 2B, right). Together with the mitotic timing results above, these results argue that the Clb2 PP is required for the normal timing of securin destruction and thus the timing of sister-chromatid separation in anaphase.

We also monitored the degradation timing of the transcriptional co-activator Ndd1. Ndd1 levels are regulated by multiple mechanisms. We showed recently that high Clb2-Cdk1 levels drive PP-dependent multisite phosphorylation of Ndd1, triggering its destruction in a prolonged spindle assembly checkpoint arrest; mutation of the Clb2 PP therefore stabilizes the protein prior to anaphase[7]. In anaphase, Ndd1 is then degraded via the Cdh1-activated form of the APC/C[36]. Here, western blotting of Ndd1 levels in cells released from a G1 arrest showed that the anaphase degradation of Ndd1, like that of securin, was delayed 10-20 minutes in the *clb2-pp* strain, and more severely delayed in *clb1*Δ *clb2-pp clb3*Δ cells (Figure 2C). These results are consistent with a delay in the onset of anaphase in *clb2-pp* cells.

Anaphase onset depends on Clb2-Cdk1-mediated multisite phosphorylation of several APC/C subunits, triggering APC/C activation by the activator subunit Cdc20[30,31,37]. A simple explanation for our results is that the Clb2 PP promotes APC/C-Cdc20 activation. We considered three possible mechanisms by which this might occur: (1) the *clb2-pp* mutation causes cytoskeletal defects that activate the morphogenesis checkpoint, resulting in suppression of Cdk1 activity by the inhibitory kinase Swe1[37]; (2) the *clb2-pp* mutation causes mitotic spindle defects that lead to APC/C inhibition by the spindle assembly checkpoint (SAC)[38,39]; or (3) the Clb2 PP is directly required for multisite phosphorylation of APC/C subunits by Cdk1[30,31].

To test whether the mitotic delay in the *clb2-pp* mutant is caused by activation of the morphogenesis checkpoint, we monitored securin degradation in strains lacking Swe1. In comparison to *swe1*Δ cells, *swe1*Δ *clb2-pp* cells displayed a mild delay in securin destruction, similar to that in *clb2-pp* cells (Figure 2D), suggesting that the small mitotic delay in *clb2-pp* cells is not due to Cdk1 inhibition by Swe1. However, deletion of *SWE1* did cause a partial reduction in the prolonged mitotic delay in *clb1*Δ *clb2-pp clb3*Δ cells, suggesting that this delay results in

part from Cdk1 inhibition by Swe1, consistent with the bud morphology defect we observe in these cells.

To test if the *clb2-pp* anaphase delay is caused by activation of the SAC, we analyzed securin levels in strains lacking Mad2, a critical SAC component[38,39]. Deletion of *MAD2* did not reduce the minor mitotic delay in *clb2-pp* cells or the lengthy delay in *clb1*Δ *clb2-pp clb3*Δ cells (Figure 2E), suggesting that SAC activation does not occur in these cells.

We next sought a genetic approach to test the possibility that the *clb2-pp* mutation directly causes defects in Cdk1-mediated APC/C phosphorylation. An ideal approach would be to test if the *clb2-pp* phenotype is rescued by an APC/C mutant that is active in the absence of phosphorylation. Such a mutant is known to be possible with the vertebrate APC/C[40–43]. In vertebrate cells, an autoinhibitory loop in the Apc1 subunit blocks Cdc20 binding in the absence of phosphorylation. Phosphorylation of other APC/C subunits (primarily Cdc27/Apc3) is thought to recruit Cdk1-cyclin B1-Cks1 via binding of Cks1 to phosphorylated residues, which leads to secondary phosphorylation of multiple sites in the autoinhibitory loop of Apc1 – thereby displacing the loop and enabling Cdc20 binding. Deletion of the autoinhibitory loop of human Apc1 results in phosphorylation-independent Cdc20 binding[40,42].

It is not known if similar mechanisms activate the budding yeast APC/C. Yeast Apc1 contains a disordered loop (aa 225-365) at the same location as the autoinhibitory loop of human Apc1, but the sequences are not related. The yeast loop contains only one Cdk1 consensus site as compared to the seven sites in the human loop. Nevertheless, we tested the possibility that deletion of this loop from yeast Apc1 rescues the anaphase defects in *clb2-pp* cells.

We constructed the *apc1-Δloop* strain, in which the *APC1* gene encodes an Apc1 protein lacking aa 225-365. This strain displayed a minor growth defect on rich media plates at 30°C or 37°C, and also on plates containing the microtubule drug benomyl (Figure S2B). A growth defect was also observed in cells grown in suspension in rich media at 30°C (Figure S2C). The timing of securin destruction in *apc1-Δloop* cells was normal (Figure 2F). The double mutant (*apc1-Δloop clb2-pp*) displayed a more severe growth phenotype on plates and in suspension (Figure S2B, S2C), as well as a severe delay in the timing of securin destruction (Figure 2G). Together, these results suggest that deletion of the Apc1 loop does not result in APC/C hyperactivation that rescues the *clb2-pp* defect; on the contrary, it seems more likely that loop deletion does not bypass the requirement for phosphorylation but simply reduces APC/C function. In this case, the synthetic defect in the double mutant is consistent with a role for the PP in APC/C function.

Phosphorylation of several proteins *in vivo* depends on the Clb2 phosphate pocket

We next used an unbiased approach to determine if the mitotic defects in *clb2-pp* cells are due to defects in Cdk1 substrate phosphorylation. We tested this possibility by quantitative mass spectrometry of protein phosphorylation in wild-type and *clb2-pp* cells, using Stable Isotope Labeling with Amino acids in Cell culture (SILAC)[44]. Wild-type and *clb2-pp* cultures were labeled differentially with “light” or “heavy” isotopes, respectively, and proteins were isolated from cell lysates and trypsinized. Phosphorylated peptides were enriched with Immobilized Metal Chelate Affinity Chromatography (IMAC) before analysis by Liquid Chromatography–Tandem Mass Spectrometry[45]. We obtained 4000 phosphopeptide sequences, of which 680 were phosphorylated at a Cdk1 consensus sequence (S/T*-P) (Table S1, Figure 3). The relative quantities of these peptides in wild-type and *clb2-pp* cells were determined, revealing 69 phosphopeptides with 2-fold or greater enrichment in the wild-type culture and 37 phosphopeptides enriched in the *clb2-pp* culture. We were particularly interested in

phosphopeptides enriched in the wild-type cells, which represent sites that are less phosphorylated in the *clb2-pp* cells, as expected for Cdk1 substrates that depend on the Clb2 PP for full phosphorylation.

Most of the potential Clb2 PP target proteins contain multiple minimal CDK consensus sequences, and several of these proteins were among the large numbers of Cdk1 substrates identified in our previous studies[1,2] (Table S2). Many of these proteins contain multiple Cdk1 consensus sites in large regions of predicted disorder, making them good candidates for PP-dependent multisite phosphorylation.

Phosphorylation of multiple CDK substrates *in vitro* depends on the Clb2 phosphate pocket

Noteworthy proteins from the list of PP-dependent phosphopeptides include Fun30 (chromatin remodeler) and Ssk1 (MAP kinase cascade component), which are highlighted in Figure 3B. Fun30 and Ssk1 contain 10 and 18 S/T*-P sites, respectively, including three optimal sites with a basic residue at the +3 position (Figure S3). To test the impact of the Clb2 PP on phosphorylation of these proteins *in vitro*, we measured phosphorylation of recombinant fragments of Fun30 (aa 1-550) and Ssk1 (aa 71-220), which are predicted to be disordered and contain multiple CDK sites as well as the phosphopeptides identified by mass spectrometry. Substrates were tested in radiolabeled kinase reactions with Cdk1-Clb2 complexes purified from yeast, carrying either wild-type Cks1 or a mutant lacking its phosphothreonine-binding site (Figure 4A, S4A, B). Reaction products were analyzed by Phos-tag SDS-PAGE, which enhances the separation of differentially phosphorylated species. Phosphorylation of Fun30 *in vitro* was not affected under these conditions by mutation of either the Clb2 or the Cks1 phospho-pocket (Figure 4A, left, S4A). However, phosphorylation of Ssk1 was reduced in the absence of the Clb2 PP but not the Cks1 phospho-pocket (Figure 5A, right, S4A). Similar to

Ndd1[7], phosphorylation of Ssk1 at early timepoints was not affected by the PP mutation, consistent with a mechanism in which the PP promotes secondary phosphorylation at later time points by interacting with initial priming site(s).

We also chose CDK substrate candidates for analysis based on the budding and anaphase defects observed in the *clb2-pp* strain. We first tested subunits of the polarisome complex, which serves as an actin-organizing center for polarized bud growth[46]. Two polarisome subunits, Spa2 and Bud6, are known to be Cdk1 targets involved in regulating budding[1,46,47]. Neither protein was identified as a PP-dependent phosphoprotein in our mass spectrometry analysis. We examined phosphorylation of disordered protein fragments from Spa2 (aa 524-670) and Bud6 (aa 126-360) (Figure S3), and observed that the Clb2 phosphate pocket is required for the multisite phosphorylation of Bud6 but not that of Spa2 (Figure 4B, S4A).

As discussed earlier, a likely explanation for the anaphase defect in *clb2-pp* cells is that the phosphate pocket is required for full phosphorylation of APC/C subunits. Three APC/C subunits, Cdc16, Cdc23, and Cdc27, as well as the large scaffolding subunit, Apc1, contain large disordered loops with numerous CDK sites, and these loops are phosphorylated during mitosis[30,31,37,42]. We therefore carried out kinase reactions *in vitro* with fragments of Cdc27 (aa 241-360) and Cdc16 (aa 1-180) (Figure S3). The Clb2 PP was required for multisite phosphorylation of both APC/C subunits (Figure 4C, S4A).

To confirm the evolutionary conservation of these mechanisms, we analyzed phosphorylation of the six yeast substrates by purified human Cdk1-cyclin B1[48,49]. Using the baculovirus expression system, we prepared recombinant complexes of human Cdk1 and cyclin B1, either wildtype or *pp* mutant (R307A, H320A, K324A). The same system was used to prepare human Cks1. The high yield of this approach allowed us to use higher concentrations of kinase in the reactions as

compared to our yeast experiments (see Methods); as a result, substrate phosphorylation was more extensive (Figure S5A, S6). As with the yeast kinase, mutation of the cyclin B1 PP inhibited phosphorylation of Ssk1, Bud6, Cdc27, and Cdc16, and had only a minimal impact on Fun30 phosphorylation. Spa2 phosphorylation by the human kinase was more PP-dependent than phosphorylation by the yeast kinase. Finally, we found that the cyclin B1 phosphate pocket is required for complete phosphorylation of a fragment of human Apc3/Cdc27 (aa 157-457) (Figure S3, S5B, S6).

In reactions with yeast or human kinases, Cks1 mutation or omission had little impact on the phosphorylation of most substrates, presumably because none of these substrates contains the optimal upstream (N-terminal) T*-P-x-K/R site that typically serves as a binding site for Cks1. On the other hand, for some substrates we observed that mutation of both Cks1 and the cyclin PP resulted in lower phosphorylation than that seen with the PP mutation alone. Thus, the two phosphate-binding sites might cooperate to promote phosphorylation at some sites.

Some aspects of Cdc16 behavior in our experiments set it apart from the other substrates. First, Cdc16 phosphorylation with human kinase resulted in higher-mobility (poorly phosphorylated) species not seen with the yeast kinase, perhaps indicating more processive modification by the yeast kinase. Second, Cdc16 phosphorylation by yeast Cdk1-Clb2 depended in part on Cks1, despite containing only one suboptimal T*-P site downstream of other potential phosphorylation sites. Further experiments will be required to unravel the mechanisms underlying these behaviors.

Discussion

Our results shed light on the biological function of the highly conserved phosphate-binding pocket (PP) of mitotic B-type cyclins. We found that mutation of the PP in budding yeast Clb2 had little impact on cell morphology or proliferation rate under normal conditions, but detailed analyses uncovered defects in the timing of anaphase onset. More pronounced defects in morphology, proliferation, and mitosis were observed when the *clb2-pp* mutation was combined with deletions of the two other major mitotic cyclin genes, *CLB1* and *CLB3*. We conclude that the PP is required for normal mitotic progression and potentially for other Clb2 functions, and that other cyclins provide some of these functions in the absence of the Clb2 PP.

The *clb2-pp* mutation, when combined with deletions of *CLB1* and *CLB3*, causes an elongated morphology that resembles the well-known bud morphology defect of *clb2*Δ cells, in which there is a delay in the switch from polar to isotropic bud growth[27,29,32]. Our results suggest that PP-dependent Clb2-Cdk1 substrates function in this switch. For example, Clb2-Cdk1 is thought to phosphorylate components of the polarisome, a protein complex that controls actin dynamics and polarized bud growth[46]. Potential Clb2-Cdk1 substrates in this complex include Spa2 and Bud6, both of which are extensively phosphorylated on multiple Cdk1 consensus sites and other sites[1,46,47]. We showed that multisite phosphorylation of Bud6 *in vitro* is highly PP-dependent, raising the possibility that the bud morphology defect in *clb2-pp* cells is due in part to reduced phosphorylation of Bud6.

Our evidence that the Clb2 PP is required for timely anaphase onset is consistent with abundant previous evidence that Cdk1 and mitotic cyclins play important roles in the metaphase-anaphase transition. Delays in anaphase onset are seen in cells carrying defects in Cdk1 activity or cyclin expression, including cells lacking *CLB2*[30,31,37,48,49]. The temperature-sensitive *clb2-IV* mutant (D232G, L286S, K353R, D485G) exhibits delayed securin degradation when

combined with a *CLB1* deletion[48]. In principle, Clb2-dependent mitotic delays might be expected to result from defects in early mitotic processes such as spindle assembly, which would delay anaphase by activation of the SAC[38,39]. However, our data suggest that the anaphase delay of the *clb2-pp* mutant is independent of the SAC.

Cdk1-dependent phosphorylation of multiple APC/C subunits is known to promote APC/C binding to the activator subunit Cdc20, thereby initiating the ubiquitination and destruction of securin and mitotic cyclins[30,31,40–43]. APC/C activation depends on multisite phosphorylation of disordered loops in conserved subunits (Cdc27, Cdc16, and Cdc23 in budding yeast). Interestingly, the Cks1 subunit is important for Cdc16 and Cdc27 hyperphosphorylation in yeast, and APC/C activation depends on Cks1-mediated APC/C hyperphosphorylation in vertebrates[30]. In this study, we observed a striking dependence on the Clb2 PP in Cdc16 and Cdc27 hyperphosphorylation *in vitro*, providing evidence that the anaphase defect in *clb2-pp* cells is due to reduced phosphorylation of APC/C subunits. We also observed that deletion of *SWE1* partially reduced the anaphase defect in *clb1*Δ *clb2-pp clb3*Δ cells, suggesting that Cdk1 catalytic activity is reduced by Swe1 in these cells, further inhibiting APC/C phosphorylation.

In vertebrates, Cks1-dependent binding of Cdk1 to APC/C subunit loops is thought to promote secondary phosphorylation on the autoinhibitory loop in the large Apc1 subunit, leading to the formation of a binding site for Cdc20[30,31,37,40,42,43,50]. However, the mechanism of APC/C activation by phosphorylation in yeast remains unclear. The sequence of the putative autoinhibitory loop of yeast Apc1 is not related to the vertebrate sequence and does not contain abundant CDK consensus sites. In a recent structural analysis of yeast APC/C, the activator binding site is not occupied by the Apc1 loop as it is in the human complex[51–53]. Our evidence does not support a role for this loop in autoinhibition. On the contrary, we found that deletion of the loop in yeast Apc1 causes a growth defect that is more severe in combination with the *clb2-*

pp mutation, suggesting that deletion of the loop reduces APC/C function. Further studies are required to decipher the mechanism by which yeast APC/C phosphorylation promotes Cdc20 binding.

Based on our phosphoproteomic studies and on the large number of Cdk1 substrates carrying multiple clustered phosphorylation sites, the *clb2-pp* phenotype is likely to be complex and arise from changes in the phosphorylation state of many proteins. For example, the high levels of Ndd1 that result from hypophosphorylation would be expected to promote changes in the expression of multiple mitotic genes. Numerous other proteins are likely to be underphosphorylated, resulting in a variety of subtle defects that are not apparent in simple studies of cell cycle progression in rich laboratory conditions. Furthermore, it is possible that the cyclin B PP is not simply involved in the enhancement of CDK substrate phosphorylation; it might also have roles in regulatory interactions. Indeed, the pocket was initially identified through its critical role in the inhibitory interaction between human Cdk1-cyclin B1 and phosphorylated separase[23]. Mutations in the phosphate pocket were found many years ago to inhibit interactions with the CDK regulator Cdc25[54]. We therefore expect that PP mutations have a broad impact on CDK function and regulation in the cell cycle.

The impact of the PP might extend beyond conventional proline-directed CDK sites. Cks1 and other docking mechanisms are known to promote non-proline directed phosphorylation by CDKs[55,56]. We speculate that the phosphate pocket in B-type cyclin has a similar function, which might explain the many PP-dependent phosphopeptides in our mass spectrometry study that did not contain a consensus S/T*-P site.

The phosphate pocket of human cyclin B1 was identified as a basic region that interacts with a specific phosphoserine in separase[23]. It is possible, however, that this basic pocket is not solely

a phosphate-binding site: it might nucleate a larger binding site for short linear sequence motifs in which an acidic residue can in some cases be used instead of a phosphate. More detailed biochemical analyses will be required to assess the precise sequence and phosphate requirements for the PP-dependent phosphorylation events we observed *in vitro*.

In summary, our evidence suggests that the phosphate pocket of B-type cyclins serves as a mechanism for promoting secondary phosphorylation of CDK substrates, similar to Cks1. This stepwise phosphorylation mechanism likely plays an important role in temporal regulation of cell cycle events[7,8,12]. Past studies have demonstrated that the timing and extent of phosphorylation depend on phosphorylation site sequence context, kinase activity level, substrate localization, cyclin-specific docking motifs, Cks1 interactions, phosphatase specificity and the positioning of phosphorylation sites. Our study adds another regulatory layer to this remarkably complex control system.

Methods

Strain and Plasmid Construction

All strains are derivatives of W303a, except that strains used for SILAC are derivatives of S288c (Table S3). Strains used in the growth assay and DIC microscopy analysis in Figure 1 were based on previously constructed *clb2-pp* strains[7]. All strains were constructed using PCR- and/or restriction digest-based homologous recombination with 50-bp flanking homology. All plasmids were constructed using Gibson assembly to recombine restriction-digested vectors with PCR products or synthetic DNA fragments (Integrated DNA Technologies, IDT) (Table S4).

Yeast Proliferation

Yeast strains were grown in YPD (1% Yeast Extract, 2% Peptone, 2% Dextrose) at 30°C unless

specified otherwise. The optical density-based growth assay was carried out using a TECAN Spark 10M plate reader. 100 µl of OD_{600}=0.05 culture was added to the wells of a transparent, sterile, flatbottom, non-tissue culture treated 96-well plate (Falcon #351172), which was then sealed with Breathe-Easy sealing membrane (Diversified Biotech #BEM-1). Absorbance (OD_{600}) of each well was measured every 15 min for 24 h during a 30°C incubation with shaking. Four replicates of each strain were analyzed. Growth rate was quantified by fitting absorbance data to a Logistic Growth Model on Prism (Graphpad). For analysis of growth on agar plates, 5 µl aliquots of 1:10 serial diluted culture from OD_{600}=0.1 were spotted and incubated at the specified temperature. A final concentration of 15 µg/ml benomyl was included in the rich media for the microtubule destabilization experiments.

Microscopy

Differential interference contrast (DIC) imaging was performed with a Nikon Ti2-E microscope and a CFI Plan Apochromat Lambda 100X/1.45 NA oil immersion objective lens. Images were captured with a Teledyne Photometrics Prime 95B 25 mm camera. Nikon NIS Elements software was used to drive stage movement and acquisition.

Live imaging of yeast cells with mCherry-tagged Spc42 was conducted as described[33]. Imaging was performed using a Nikon Ti-E microscope equipped with a Yokogawa CSU-22 spinning disk confocal unit and a Teledyne Photometrics Evolve EMCCD camera (UCSF Center for Advanced Light Microscopy). Imaging sessions typically lasted 1.5 h with 2 min between frames. For each time point and channel, z-stacks were acquired across a distance of 5 µm with 0.5 µm steps. The exposure time for the mCherry channel was set to be less than 40 ms for each z-slice. The imaging system was controlled using Nikon NIS Elements software, ensuring precise and accurate acquisition of the images.

Prior to fluorescence microscopy, yeast were grown for 24 h in synthetic complete media with 2% glucose (SD), with dilution to maintain OD_{600} <0.4. For imaging, wells in a 96-well Glass Bottom Microwell Plate (MGB096-1-2-LG-L) were pre-treated with 10 mg/ml Concanavalin A for 1 h and washed with water. 100 µl cell culture was added and immobilized 40–60 min in a 30°C incubator. Unattached cells were washed off with fresh media before imaging. To minimize autofluorescence, all media was filtered instead of autoclaved.

SILAC Mass Spectrometry

SD-Arg-Lys media is made with a premixed CSM-Arg-Lys drop out powder (Sunrise Science Products). To make a 1000x stock solution of lysine and arginine (30 mg/ml lysine, 20 mg/ml arginine), L-lysine-HCl (Sigma #L5626) and L-arginine-HCl (Sigma #A5131) were dissolved in water and filter-sterilized with a 0.2 µm filter. Heavy arginine and lysine contain the isotopes ^{13}C and ^{15}N: L-lysine:2HCl (Cambridge Isotope #CNLM-291-H) and L-arginine:HCl (Cambridge isotope # CNLM-539-H).

Wild-type and *clb2-pp* strains were grown in 2 liters SD + 2% Dextrose + 2 ml heavy or light amino acid stock to OD_{600} = 0.5. Harvested cells were washed, resuspended in 50 ml lysis buffer (100 mM Tris-HCl pH 8.0, 2% SDS) and snap frozen as “popcorn” by dropwise freezing in liquid N_2. Frozen cell suspensions were lysed in a cryomill (SPEX SamplePrep 6870). The frozen milled powder was quickly heated to 60°C and incubated for 30 min, followed by centrifugation at 15000x g for 10 min to remove cell debris. Lysate was incubated with 10 mM DTT at 60°C for 30 min, then alkylated with 30 mM iodoacetate at room temperature for 30 min in the dark. Proteins were precipitated using ethanol/acetone and washed three times with 40% ethanol/40% acetone, then stored at -20°C before solubilization and trypsin digestion.

Protein pellets were dissolved in 20 ml 8 M urea in 50 mM Tris-HCl pH 8.0 with a dounce homogenizer, and centrifuged at 4000x g for 10 min. The supernatant was diluted 5-fold with 50 mM Tris-HCl pH 8.0 and digested for 12 h at 37°C using sequencing grade trypsin (Promega cat#: V511A) at 1/100 the mass of total protein. Tryptic digests were acidified to a final concentration of 0.5% Trifluoracetic acid (TFA) and centrifuged at 4000x g. Solid phase extraction was performed using a 5 g Sep-Pak C18 column (Waters #WAT036925) as follows: columns were pre-washed with 1 column volume (20 ml) of methanol, followed by 1 column volume of 80% acetonitrile:0.1% TFA, and equilibrated using 2 column volumes of 0.1% TFA. Tryptic digests were loaded by gravity flow and washed with two column volumes of 0.1% acetic acid. Peptides were eluted using 1.5 column volumes of 80% acetonitrile, 0.1% acetic acid, and dried under centrifugation and vacuum.

Phosphopeptides were purified by Fe^{3+}-nitrilotriacetic acid immobilized metal affinity chromatography (IMAC) silica resin as described previously[57]. Dried peptides were resuspended in 0.6% acetic acid (10 µg/µl peptide concentration) and centrifuged for 5 min at 2300x g. Supernatant was loaded onto a microcapillary column containing freshly prepared IMAC resin and washed twice with 60 µl wash buffer containing 25% acetonitrile, 100 mM NaCl, and 0.1% acetic acid, once with 60 µl 0.1% acetic acid, and once with 30 µl water. Loading and washing was performed using a syringe at a flow rate of 1 to 2 µl/min. Phosphopeptides were eluted into a glass insert with 180 µl 6% NH_4OH and dried under vacuum. Dried phosphopeptides were stored at −20°C.

Phosphopeptides were directly analyzed following reconstitution in 0.6% acetic acid by autosampler injection onto a liquid chromatography system coupled to a high-resolution mass spectrometer (Thermo Scientific UltiMate 3000 RSLCnano, Orbitrap Fusion Lumos) operated in data dependent mode. Data analysis was performed using the COMET database search tool

that is part of the Trans Proteomic Pipeline (TPP) software suite. Search results were then processed and quantified using the XPRESS component of TPP to generate SILAC ratios of the identified phosphorylated peptides. A false discovery rate of less than 1% was applied for the identified phosphopeptides, combined with manual interrogation of MS/MS spectra and parent ion chromatograms as a final quality control for identification and quantification, respectively.

Protein Purification

Wild-type and *clb2-pp* Cdk1-Clb2 complexes were purified as described[1,58]. Briefly, TAP-tagged *CLB2* was overexpressed from a 2-micron *URA3* plasmid under *GAL* control. Yeast were grown in SD-Ura + 2% raffinose at 30°C with shaking to OD_{600}=0.6, followed by induction with 2% galactose for 2 h. Cells were harvested, washed with PBS, and resuspended in 10 ml of TAP lysis buffer (25 mM HEPES pH 8.0, 1 M NaCl, 0.1% NP-40, 1 mM EDTA, 30 mM EGTA, 1 mM PMSF, 1 cOmplete Protease Inhibitor Tablet, 80 mM beta-glycerophosphate, 50 mM NaF, 1 mM Na_3VO_4). Cells were frozen in liquid N_2 and stored at -80ºC. Frozen cells and 50 ml of lysis buffer pellets were processed in a cryomill (SPEX SamplePrep 6870) for 8 cycles of 2-min grinding followed by 2 min chilling. Lysate was clarified by centrifugation at 10,000 rpm (Beckman Ti45 rotor) and then 50,000 rpm (Beckman Ti70 rotor), and bound to IgG Sepharose 6 Fast Flow beads (GE 52-2083-00 AH) for 1 h at 4ºC. The column was washed 3 times with 10 bed volumes of TAP lysis buffer and 1 volume of TEV cleavage buffer (10 mM Tris-HCl pH 8.0, 150 mM NaCl, 0.1% NP-40, 0.5 mM EDTA, 1 mM DTT). Cdk1-Clb2 complexes were cleaved off the column with AcTEV (Invitrogen Cat#12575015) in 1 ml TEV cleavage buffer for 90 min at 16°C. Eluate was collected by passing an additional 400 µl TEV cleavage buffer over the column. AcTEV was removed by incubation with Ni-NTA beads (QIAGEN #30230) for 1 h at 16°C. The eluate was concentrated in centrifugal concentrators (Millipore Sigma #UFC803024) and stored in 10% glycerol at -80°C.

Purification of recombinant wild-type and mutant *S. cerevisiae* Cks1 was performed as described[20] with the following modifications. Briefly, BL21(DE3) Star cells transformed with a plasmid expressing *CKS1* from the T7 promoter were grown in 1 liter of LB + Amp at 37°C to an OD_{600} of 0.6, then induced with 1 mM IPTG at 16°C overnight. Cells were frozen in liquid N_2, thawed, sonicated in 10 ml phosphate-buffered saline, and clarified by centrifugation at 7000 rpm (Beckman Ti45 rotor). Supernatant was incubated in a boiling water bath for 5 min and centrifuged for 10 min at 40,000 rpm (Beckman Ti45 rotor). Supernatant was supplemented with ammonium sulfate (1 g per 6.1 ml), incubated for 30 min at 4°C, and centrifuged at 40,000 rpm for 10 min (Beckman Ti45 rotor). The pellet was redissolved in 10 ml Tris-NaCl-EDTA buffer (50 mM Tris pH 7.5, 100 mM NaCl, 2 mM EDTA) and dialyzed against three changes of Tris-NaCl buffer (50 mM Tris pH 7.5, 100 mM NaCl). Dialysate was subjected to gel filtration on a S200 column, and fractions containing Cks1 were pooled and concentrated in a 15-ml Millipore centrifugal concentrator (nominal molecular mass cutoff = 10 kDa).

For production of CDK substrates, a codon-optimized synthetic DNA (IDT) was inserted into a pET28 expression vector by Gibson assembly, fused to DNA encoding an N-terminal 6xHis-SUMO or 6xHis-GST-TEV tag. BL21(DE3) Star cells transformed with plasmids expressing recombinant protein from the T7 promoter were grown in 2 liter of LB + Kan at 37°C to an OD_{600} of 0.6, then induced with 1 mM of IPTG at 16°C overnight. Cells were frozen in liquid N_2. Depending on protein expression level, substrates were purified under native (Ssk1 and hApc3) or denaturing conditions (Fun30, Spa2, Bud6, Cdc27 and Cdc16). In a native purification, cell pellets were thawed and resuspended in native His lysis buffer (50 mM Tris pH 7.5, 300 mM NaCl, 20 mM Imidazole, 3 mM DTT, 5% Glycerol) supplemented with 250 U of DNAseI, 250 U of Benzonase, 1 cOmplete Protease Inhibitor Tablet, 500 µg/ml lysozyme and 1 mM PMSF. Suspended cells were lysed via an LM10 (Microfluidics) microfluidizer, twice at 12,000 psi. Lysate was then clarified by centrifugation at 40,000 rpm for 30 min (Beckman Ti45 rotor).

Supernatant was incubated with Ni-NTA beads (QIAGEN #30230) for 1 h at 16°C. The beads were washed 3 times with 10 bed volumes of native His lysis buffer, and eluted with 4 ml 200 mM imidazole in the same buffer. The eluate was subjected to gel filtration on a S200 column, and fractions containing appropriately sized proteins were pooled and concentrated in a 4-ml Millipore centrifugal concentrator (nominal molecular mass cutoff = 10, 30 or 50 kDa) before being snap frozen in liquid N_2. Denaturing purifications were performed as previously described[59]. In brief, cell pellets were thawed and resuspended in denaturing lysis buffer (50 mM HEPES pH 7.5, 500 mM NaCl, 20 mM imidazole, 6M urea, 0.5 mM TCEP, 10% glycerol), followed by purification on Ni-NTA beads as above except in denaturing lysis buffer. Eluate was dialyzed to remove urea before gel filtration.

Wild-type and mutant human Cdk1-cyclin B1 complexes were expressed from recombinant baculoviruses and purified as previously described[59]. Human Cks1 was expressed from a recombinant baculovirus encoding a His-TEV-Cks1 fusion, and purified as described[60] with the following modifications. In brief, 800 ml of infected SF-900 cells were harvested and resuspended in buffer A (50 mM HEPES pH 7.4, 250 mM NaCl, 15 mM imidazole, 2 mM TCEP, 5% glycerol) supplemented with 250 U of Benzonase and 1 cOmplete Protease Inhibitor Tablet. After sonication, the lysate was centrifuged at 50,000 rpm (Beckman Ti70 rotor) for 1 h at 4°C. Supernatant was loaded onto Ni-NTA beads (QIAGEN #30230) and eluted using 250 mM imidazole. Eluate was incubated with AcTEV (Invitrogen Cat#12575015) to remove the His tag and was dialyzed overnight in buffer A to remove excess imidazole. Cleaved Cks1 was reapplied to Ni-NTA beads to remove the AcTEV; the flowthrough was concentrated and subjected to gel filtration on a S75 column. Fractions containing Cks1 were pooled and concentrated in a 4-ml Millipore centrifugal concentrator (nominal molecular mass cutoff = 3 kDa) before snap freezing.

Kinase Assays

All substrates were buffer exchanged into 50 mM HEPES pH 7.5, 50 mM NaCl, 0.5 mM TCEP, 10% glycerol. Kinase reactions with yeast Cdk1-Clb2 were performed as previously described[7]. Briefly, prior to adding substrates, ~1-5 nM CDK complexes and 200 nM Cks1 were incubated in the presence of 10 mM $MgCl_2$ and 100 μM ATP for 45 min. Phosphorylation reactions were initiated by combining 25 nCi [γ-^{32}P]-ATP (Hartmann Analytic) and 1-2 μg of substrate with the CDK-Cks1 mixture in kinase buffer (25 mM HEPES pH 7.5, 50 mM NaCl 10 mM $MgCl_2$, 1 mM DTT, 100 μM ATP) and incubated at 25°C. Reactions were arrested at specific time points by addition to SDS-PAGE sample buffer, and products were analyzed by Phos-tag SDS-PAGE with a gel composition of either 6 or 7.5% acrylamide and 50 μM Phos-tag (Wako Chemicals). Autoradiography was performed with an Amersham Typhoon 5 Biomolecular Imager (GE Healthcare Life Sciences), and images were quantified using ImageQuant TL software (Amersham Biosciences). Phosphorylation reactions with human kinase were performed similarly except with 100 nM final concentration of CDK.

Western Blotting

Yeast strains expressed C-terminally Myc-tagged proteins either at the endogenous locus (securin) or at the *TRP1* locus under the control of the *GAL* promoter (Ndd1)[7]. For *GAL*-induced *NDD1* expression, galactose was added to a final concentration of 2% in YEP-raffinose medium. Cells were arrested by alpha factor (1.5 μg/ml) for 3 h at 30°C and released from arrest by washing 3 times with fresh media. Samples (1 ml) were harvested at 20-min intervals after release. To block entry into the following cell cycle, alpha factor was added back to the culture 1 h after release, when most cells had budded. Yeast lysates were prepared by bead-beating cells for 2 min in 100 μl urea lysis buffer (20 mM Tris-HCl pH 7.4, 7 M urea, 2 M thiourea, 65 mM CHAPS, 10 mM DTT). Following SDS-PAGE of lysates, proteins were transferred to 0.45-micron nitrocellulose membrane (GE-Healthcare Life Sciences) at a constant

voltage of 110V for 70 min at 4°C. Blots were incubated overnight at 4°C with primary antibodies: either mouse anti-Myc (9B11 Cell Signaling Technology) diluted 1:5000, or GAPDH monoclonal antibody (GA1R Thermo) diluted 1:2500 in TBS-T containing 4% nonfat dry milk. After washing, blots were incubated at room temperature for 1 h with secondary antibody IRDye 800CW Donkey anti-Mouse IgG (926-32212 LI-COR), diluted 1:2000 in TBS-T. After washing, fluorescence signals on the blots were captured using an Odyssey Fc imager (LI-COR) at 800 nm for a duration of 10 min.

Acknowledgments

We thank Chris Carlson, Chloe Ghent, Briana Marinoni, Emmy Delaney, Jonah Goodfried, Mart Loog, David Barford, Andreas Boland, and Thomas Mayer for helpful discussions, Haley Gause and Kari Herrington for assistance with microscopy, and Sandra Catania for assistance with sample preparation for SILAC-MS. This work was supported by grants from the National Institute of General Medical Sciences: R35-GM118053 (D.O.M.) and R01-GM151191 (R.T.S. and H.Z.). Fluorescence microscopy was performed at the UCSF Center of Advanced Light Microscopy, with support from a NIH S10 Shared Instrumentation grant (1S10OD017993-01A1).

Author contributions

H.Y.N. conceived the project, performed experiments and analyzed results, with assistance from A.N.A. and D.H.W. and guidance from D.O.M. R.T.S. and H.Z. performed mass spectrometry analyses. H.Y.N. and D.O.M. wrote the paper with assistance from all other authors.

Declaration of interests

The authors declare no competing interests.

References

1. Ubersax, J.A., Woodbury, E.L., Quang, P.N., Paraz, M., Blethrow, J.D., Shah, K., Shokat, K.M., and Morgan, D.O. (2003). Targets of the cyclin-dependent kinase Cdk1. Nature *425*, 859–864. 10.1038/nature02062.
2. Holt, L.J., Tuch, B.B., Villen, J., Johnson, A.D., Gygi, S.P., and Morgan, D.O. (2009). Global analysis of Cdk1 substrate phosphorylation sites provides insights into evolution. Science (1979) *325*, 1682–1686. 10.1126/science.1172867.
3. Loog, M., and Morgan, D.O. (2005). Cyclin specificity in the phosphorylation of cyclin-dependent kinase substrates. Nature *434*, 104–108. 10.1038/nature03329.
4. Coudreuse, D., and Nurse, P. (2010). Driving the cell cycle with a minimal CDK control network. Nature *468*, 1074–1079. 10.1038/nature09543.
5. Swaffer, M.P., Jones, A.W., Flynn, H.R., Snijders, A.P., and Nurse, P. (2016). CDK Substrate Phosphorylation and Ordering the Cell Cycle. Cell *167*, 1750–1761. e16. 10.1016/j.cell.2016.11.034.
6. Wittenberg, C., and Reed, S.I. (2005). Cell cycle-dependent transcription in yeast: promoters, transcription factors, and transcriptomes. Oncogene *24*, 2746–2755. 10.1038/sj.onc.1208606.
7. Asfaha, J.B., Örd, M., Carlson, C.R., Faustova, I., Loog, M., and Morgan, D.O. (2022). Multisite phosphorylation by Cdk1 initiates delayed negative feedback to control mitotic transcription. Curr Biol *32*, 256-263.e4. 10.1016/j.cub.2021.11.001.
8. Kõivomägi, M., Valk, E., Venta, R., Iofik, A., Lepiku, M., Balog, E.R.M., Rubin, S.M., Morgan, D.O., and Loog, M. (2011). Cascades of multisite phosphorylation control Sic1 destruction at the onset of S phase. Nature *480*, 128–131. 10.1038/nature10560.
9. Ercan, D.P., Chretien, F., Chakravarty, P., Flynn, H.R., Snijders, A.P., and Uhlmann, F. (2021). Budding yeast relies on G1 cyclin specificity to couple cell cycle progression with morphogenetic development. Sci Adv *7*, eabg0007. 10.1126/sciadv.abg0007.

10. Bhaduri, S., and Pryciak, P.M. (2011). Cyclin-specific docking motifs promote phosphorylation of yeast signaling proteins by G1/S Cdk complexes. Current Biology *21*, 1615–1623. 10.1016/j.cub.2011.08.033.

11. Örd, M., Venta, R., Möll, K., Valk, E., and Loog, M. (2019). Cyclin-Specific Docking Mechanisms Reveal the Complexity of M-CDK Function in the Cell Cycle. Mol Cell *75*, 76–89. e3. 10.1016/j.molcel.2019.04.026.

12. Valk, E., Venta, R., Örd, M., Faustova, I., Kõivomägi, M., and Loog, M. (2014). Multistep phosphorylation systems: tunable components of biological signaling circuits. Mol Biol Cell *25*, 3456–3460. 10.1091/mbc.E14-02-0774.

13. Kõivomägi, M., Örd, M., Iofik, A., Valk, E., Venta, R., Faustova, I., Kivi, R., Balog, E.R.M., Rubin, S.M., and Loog, M. (2013). Multisite phosphorylation networks as signal processors for Cdk1. Nat Struct Mol Biol *20*, 1415–1424. 10.1038/nsmb.2706.

14. Mochida, S., and Hunt, T. (2012). Protein phosphatases and their regulation in the control of mitosis. EMBO Rep *13*, 197–203. 10.1038/embor.2011.263.

15. Godfrey, M., Touati, S.A., Kataria, M., Jones, A., Snijders, A.P., and Uhlmann, F. (2017). PP2ACdc55 Phosphatase Imposes Ordered Cell-Cycle Phosphorylation by Opposing Threonine Phosphorylation. Mol Cell *65*, 393-402 e3. 10.1016/j.molcel.2016.12.018.

16. Kamenz, J., and Ferrell Jr., J.E. (2017). The Temporal Ordering of Cell-Cycle Phosphorylation. Mol Cell *65*, 371–373. 10.1016/j.molcel.2017.01.025.

17. Nguyen, H., and Kettenbach, A.N. (2023). Substrate and phosphorylation site selection by phosphoprotein phosphatases. Trends Biochem Sci *48*, 713–725. 10.1016/j.tibs.2023.04.004.

18. Holder, J., Poser, E., and Barr, F.A. (2019). Getting out of mitosis: spatial and temporal control of mitotic exit and cytokinesis by PP1 and PP2A. FEBS Lett *593*, 2908–2924. 10.1002/1873-3468.13595.

19. Hein, J.B., Hertz, E.P.T., Garvanska, D.H., Kruse, T., and Nilsson, J. (2017). Distinct kinetics of serine and threonine dephosphorylation are essential for mitosis. Nat Cell Biol *19*, 1433–1440. 10.1038/ncb3634.

20. Reynard, G.J., Reynolds, W., Verma, R., and Deshaies, R.J. (2000). Cks1 is required for G(1) cyclin-cyclin-dependent kinase activity in budding yeast. Mol Cell Biol *20*, 5858–5864. 10.1128/MCB.20.16.5858-5864.2000.

21. Hadwiger, J.A., Wittenberg, C., Mendenhall, M.D., and Reed, S.I. (1989). The *Saccharomyces cerevisiae CKS1* Gene, a Homolog of the *Schizosaccharomyces pombe suc1* $^{+}$ Gene, Encodes a Subunit of the Cdc28 Protein Kinase Complex. Mol Cell Biol *9*, 2034–2041. 10.1128/mcb.9.5.2034-2041.1989.

22. Tang, Y., and Reed, S.I. (1993). The Cdk-associated protein Cks1 functions both in G1 and G2 in Saccharomyces cerevisiae. Genes Dev. *7*, 822–832. 10.1101/gad.7.5.822.

23. Yu, J., Raia, P., Ghent, C.M., Raisch, T., Sadian, Y., Cavadini, S., Sabale, P.M., Barford, D., Raunser, S., Morgan, D.O., et al. (2021). Structural basis of human separase regulation by securin and CDK1-cyclin B1. Nature *596*, 138–142. 10.1038/s41586-021-03764-0.

24. McGrath, D.A., Balog, E.R.M., Kõivomägi, M., Lucena, R., Mai, M. V, Hirschi, A., Kellogg, D.R., Loog, M., and Rubin, S.M. (2013). Cks confers specificity to phosphorylation-dependent CDK signaling pathways. Nat Struct Mol Biol *20*, 1407–1414. 10.1038/nsmb.2707.

25. Örd, M., Möll, K., Agerova, A., Kivi, R., Faustova, I., Venta, R., Valk, E., and Loog, M. (2019). Multisite phosphorylation code of CDK. Nat Struct Mol Biol *26*, 649–658. 10.1038/s41594-019-0256-4.

26. Reynolds, D., Shi, B.J., McLean, C., Katsis, F., Kemp, B., and Dalton, S. (2003). Recruitment of Thr 319-phosphorylated Ndd1p to the FHA domain of Fkh2p requires Clb

kinase activity: a mechanism for CLB cluster gene activation. Genes Dev *17*, 1789–1802. 10.1101/gad.1074103.

27. Eluere, R., Offner, N., Varlet, I., Motteux, O., Signon, L., Picard, A., Bailly, E., and Simon, M.N. (2007). Compartmentalization of the functions and regulation of the mitotic cyclin Clb2 in S. cerevisiae. J Cell Sci *120*, 702–711. 10.1242/jcs.03380.

28. Wäsch, R., and Cross, F. (2002). APC-dependent proteolysis of the mitotic cyclin Clb2 is essential for mitotic exit. Nature *418*, 556-62. 10.1038/nature00856.

29. Richardson, H., Lew, D.J., Henze, M., Sugimoto, K., and Reed, S.I. (1992). Cyclin-B homologs in Saccharomyces cerevisiae function in S phase and in G2. Genes Dev *6*, 2021–2034. 10.1101/gad.6.11.2021.

30. Rudner, A.D., and Murray, A.W. (2000). Phosphorylation by Cdc28 activates the Cdc20-dependent activity of the anaphase-promoting complex. J. Cell Biol. *149*, 1377–1390. 10.1083/jcb.149.7.1377.

31. Rudner, A.D., Hardwick, K.G., and Murray, A.W. (2000). Cdc28 activates exit from mitosis in budding yeast. J Cell Biol *149*, 1361–1376. 10.1083/jcb.149.7.1361.

32. Lew, D.J., and Reed, S.I. (1993). Morphogenesis in the yeast cell cycle: regulation by Cdc28 and cyclins. J Cell Biol *120*, 1305–1320. 10.1083/jcb.120.6.1305.

33. Lu, D., Hsiao, J.Y., Davey, N.E., Van Voorhis, V.A., Foster, S.A., Tang, C., and Morgan, D.O. (2014). Multiple mechanisms determine the order of APC/C substrate degradation in mitosis. J Cell Biol *207*, 23–39. 10.1083/jcb.201402041.

34. Jaspersen, S.L., Huneycutt, B.J., Giddings Jr., T.H., Resing, K.A., Ahn, N.G., and Winey, M. (2004). Cdc28/Cdk1 regulates spindle pole body duplication through phosphorylation of Spc42 and Mps1. Dev Cell *7*, 263–274. 10.1016/j.devcel.2004.07.006.

35. Castillo, A.R., Meehl, J.B., Morgan, G., Schutz-Geschwender, A., and Winey, M. (2002). The yeast protein kinase Mps1p is required for assembly of the integral spindle pole body component Spc42p. J Cell Biol *156*, 453-65. 10.1083/jcb.200111025.

36. Sajman, J., Zenvirth, D., Nitzan, M., Margalit, H., Simpson-Lavy, K.J., Reiss, Y., Cohen, I., Ravid, T., and Brandeis, M. (2015). Degradation of Ndd1 by APC/C(Cdh1) generates a feed forward loop that times mitotic protein accumulation. Nat Commun *6*, 7075. 10.1038/ncomms8075.

37. Lianga, N., Williams, E.C., Kennedy, E.K., Dore, C., Pilon, S., Girard, S.L., Deneault, J.S., and Rudner, A.D. (2013). A Wee1 checkpoint inhibits anaphase onset. J Cell Biol *201*, 843–862. 10.1083/jcb.201212038.

38. Musacchio, A. (2015). The Molecular Biology of Spindle Assembly Checkpoint Signaling Dynamics. Curr Biol *25*, R1002-18. 10.1016/j.cub.2015.08.051.

39. McAinsh, A.D., and Kops, G.J.P.L. (2023). Principles and dynamics of spindle assembly checkpoint signalling. Nat Rev Mol Cell Biol *24*, 543–559. 10.1038/s41580-023-00593-z.

40. Qiao, R., Weissmann, F., Yamaguchi, M., Brown, N.G., VanderLinden, R., Imre, R., Jarvis, M.A., Brunner, M.R., Davidson, I.F., Litos, G., et al. (2016). Mechanism of APC/CCDC20 activation by mitotic phosphorylation. Proc Natl Acad Sci U S A *113*, E2570-8. 10.1073/pnas.1604929113.

41. Fujimitsu, K., Grimaldi, M., and Yamano, H. (2016). Cyclin-dependent kinase 1-dependent activation of APC/C ubiquitin ligase. Science *352*, 1121–1124. 10.1126/science.aad3925.

42. Zhang, S., Chang, L., Alfieri, C., Zhang, Z., Yang, J., Maslen, S., Skehel, M., and Barford, D. (2016). Molecular mechanism of APC/C activation by mitotic phosphorylation. Nature *533*, 260–264. 10.1038/nature17973.

43. Alfieri, C., Zhang, S., and Barford, D. (2017). Visualizing the complex functions and mechanisms of the anaphase promoting complex/cyclosome (APC/C). Open Biol *7*. 10.1098/rsob.170204.

44. Ong, S.-E., Blagoev, B., Kratchmarova, I., Kristensen, D.B., Steen, H., Pandey, A., and Mann, M. (2002). Stable isotope labeling by amino acids in cell culture, SILAC, as a

simple and accurate approach to expression proteomics. Mol Cell Proteomics *1*, 376–386. 10.1074/mcp.m200025-mcp200.

45. Villen, J., and Gygi, S.P. (2008). The SCX/IMAC enrichment approach for global phosphorylation analysis by mass spectrometry. Nat Protoc *3*, 1630–1638. nprot.2008.150 [pii] 10.1038/nprot.2008.150.

46. Wang, H., Huang, Z.-X., Au Yong, J.Y., Zou, H., Zeng, G., Gao, J., Wang, Y., Wong, A.H.-H., and Wang, Y. (2016). CDK phosphorylates the polarisome scaffold Spa2 to maintain its localization at the site of cell growth. Mol Microbiol *101*, 250–264. 10.1111/mmi.13386.

47. Xie, Y., and Miao, Y. (2021). Polarisome assembly mediates actin remodeling during polarized yeast and fungal growth. J Cell Sci *134*. 10.1242/jcs.247916.

48. Rahal, R., and Amon, A. (2008). Mitotic CDKs control the metaphase-anaphase transition and trigger spindle elongation. Genes Dev *22*, 1534–1548. 10.1101/gad.1638308.

49. Lianga, N., Doré, C., Kennedy, E.K., Yeh, E., Williams, E.C., Fortinez, C.M., Wang, A., Bloom, K.S., and Rudner, A.D. (2018). Cdk1 phosphorylation of Esp1/Separase functions with PP2A and Slk19 to regulate pericentric Cohesin and anaphase onset. PLoS Genet *14*, e1007029. 10.1371/journal.pgen.1007029.

50. Li, Q., Chang, L., Aibara, S., Yang, J., Zhang, Z., and Barford, D. (2016). WD40 domain of Apc1 is critical for the coactivator-induced allosteric transition that stimulates APC/C catalytic activity. Proc Natl Acad Sci U S A *113*, 10547–10552. 10.1073/pnas.1607147113.

51. Barford, D., Vazquez-Fernandez, E., Zhang, Z., and Yang, J. (2022). S. cerevisiae APC/C-Cdh1 complex. 10.2210/pdb8a3t/pdb.

52. Barford, D., Fernandez-Vazquez, E., Zhang, Z., and Yang, J. (2022). S. cerevisiae apo unphosphorylated APC/C. 10.2210/pdb8a5y/pdb.

53. Barford, D., Fernandez-Vazquez, E., Zhang, Z., and Yang, J. (2022). S. cerevisiae apo phosphorylated APC/C. 10.2210/pdb8a61/pdb.

54. Goda, T., Ishii, T., Nakajo, N., Sagata, N., and Kobayashi, H. (2003). The RRASK motif in Xenopus cyclin B2 is required for the substrate recognition of Cdc25C by the cyclin B-Cdc2 complex. Journal of Biological Chemistry *278*, 19032–19037. 10.1074/jbc.M300210200.

55. Al-Rawi, A., Kaye, E., Korolchuk, S., Endicott, J.A., and Ly, T. (2023). Cyclin A and Cks1 promote kinase consensus switching to non-proline-directed CDK1 phosphorylation. Cell Rep *42*, 112139. 10.1016/j.celrep.2023.112139.

56. Valk, E., Örd, M., Faustova, I., and Loog, M. (2023). CDK signaling via nonconventional CDK phosphorylation sites. Mol Biol Cell *34*, pe5. 10.1091/mbc.E22-06-0196.

57. Suhandynata, R., Liang, J., Albuquerque, C.P., Zhou, H., and Hollingsworth, N.M. (2014). A method for sporulating budding yeast cells that allows for unbiased identification of kinase substrates using stable isotope labeling by amino acids in cell culture. G3 (Bethesda) *4*, 2125–2135. 10.1534/g3.114.013888.

58. Puig, O., Caspary, F., Rigaut, G., Rutz, B., Bouveret, E., Bragado-Nilsson, E., Wilm, M., and Seraphin, B. (2001). The tandem affinity purification (TAP) method: a general procedure of protein complex purification. Methods *24*, 218–229. 10.1006/meth.2001.1183.

59. Carlson, C.R., Asfaha, J.B., Ghent, C.M., Howard, C.J., Hartooni, N., Safari, M., Frankel, A.D., and Morgan, D.O. (2020). Phosphoregulation of Phase Separation by the SARS-CoV-2 N Protein Suggests a Biophysical Basis for its Dual Functions. Mol Cell *80*, 1092-1103.e4. 10.1016/j.molcel.2020.11.025.

60. Huis In ’t Veld, P.J., Wohlgemuth, S., Koerner, C., Müller, F., Janning, P., and Musacchio, A. (2022). Reconstitution and use of highly active human CDK1:Cyclin-B:CKS1 complexes. Protein Sci *31*, 528–537. 10.1002/pro.4233.

Figure legends

Figure 1. Mutation of the conserved phosphate-binding pocket in Clb2 causes a growth defect in the absence of *CLB1* and *CLB3*.

A. Aligned amino acid sequences of B-type cyclins, with cyan indicating the three basic residues that constitute the phosphate-binding pocket. These residues are not conserved in A-type cyclins.

B. (left) Growth curves of indicated yeast strains, with OD_{600} recorded every 15 min. Data represent mean ± standard deviation (SD) of four independent biological replicates. (right) Growth rates calculated by fitting OD_{600}/min to a logistic growth model. Data represent mean ± SD of four independent biological replicates. Statistical significance was determined using one-way analysis of variance (ANOVA) (****$p < 0.0001$).

C. Representative differential interference contrast (DIC) microscopy images of the indicated yeast strains at mid-log phase in rich (YPD) media at 30°C. Scale bar is 10 µm.

Figure 2. The *clb2-pp* mutation causes a mitotic delay.

A. Single-cell measurements of time from SPB separation to spindle elongation in asynchronous wild-type (WT) or *clb2-pp* cells carrying mCherry-labeled Spc42. Each data point represents a single cell and the bars indicate median ± SD. The sample size (n) is noted at right. See Figure S2A for representative images.

B. Western blots of Myc-tagged securin after release from a G1 arrest in the indicated yeast strains. Alpha factor was added back at the 60-min time point. GAPDH loading control on lower blot. Representative of 10 independent experiments.

C. Western blots of Myc-tagged Ndd1 after release from a G1 arrest in the indicated yeast strains. These strains carry a second copy of Ndd1-Myc under the control of a *GAL* promoter, and experiments were performed in galactose media. Alpha factor was added back at the 60-min time point. GAPDH loading control on lower blot. Representative of 2 independent experiments.

D. Same as B with *swe1*Δ. Representative of 2 independent experiments.

E. Same as B with *mad2*Δ. Representative of 2 independent experiments.

F. Same as B with *apc1-*Δ*loop*. Representative of 2 independent experiments.

Figure 3. Identification of proteins with reduced phosphorylation in *clb2-pp* cells.

A. Identification of IMAC-purified phosphopeptides in the SILAC-MS experiment comparing log-phase wild-type cells in 'light' media with *clb2-pp* cells in 'heavy' media (see Table S1). Each dot represents a single phosphopeptide, plotted according to its total abundance (y-axis; summed peak areas of heavy and light peptides) and the Log_2 of the ratio of light peak areas:heavy peak areas (L/H) peptide abundance (x-axis). Log_2 L/H ratios above +1 represent phospho-peptides that were appreciably reduced in *clb2-pp* cells, as expected for phosphorylation sites that depend on the Clb2 PP.

B. Plot of the subset of phosphopeptides in which the identified phosphorylation site lies in a CDK consensus site (S/T*-P). Peptides from two putative CDK substrates are labeled.

Figure 4. Phospho-pocket mutations reduce phosphorylation of multiple CDK substrates *in vitro*.

A. Purified fragments of Fun30 (aa 1-550) and Ssk1 (aa 71-220) were incubated with wild-type or *clb2-pp* Clb2-Cdk1 plus wild-type or mutant Cks1 and radiolabeled ATP. Reaction products were analyzed by Phos-tag SDS-PAGE and autoradiography. Diagrams at top

indicate optimal (S/T*-P-x-K/R; green) and suboptimal (S/T*-P; yellow) CDK consensus sites in the tested fragment (see Figure S3 for complete sequences). Total radioactive signal in each lane was quantified and normalized to maximum intensity (%). Representative of 3 independent experiments. Coomassie Blue-stained gels shown in Figure S4.

B. Same as A with fragments of the polarisome components Spa2 (aa 524-670) and Bud6 (aa 126-360). Representative of 2 independent experiments.

C. Same as A with fragments of the APC/C subunits Cdc27 (aa 241-360) and Cdc16 (aa 1-180). Representative of 2 independent experiments.

Figure 1

A

Saccharomyces cerevisiae	Clb1	346	RRISKADDYDIQSRTLAK	363
	Clb2	366	RRISKADDYDIQSRTLAK	383
	Clb3	306	RRISKADDYEHDTRTLAK	323
	Clb4	345	RRISKADDYDFEPRTLAK	362
	Clb5	303	RRISKADDYDPVNRNIGK	320
	Clb6	261	RRISKADNYCIETRNMAK	278
Schizosaccharomyces pombe	Cdc13	341	RRISKADFYDIQTRTVAK	358
Homo sapiens	Ccnb1	307	RRASKIGEVDVEQHTLAK	324
	Ccnb2	271	RRASKAGEVDVEQHTLAK	288
	Ccnb3	1266	RRYARCIHTNMKTLTLSR	1283
Mus musculus	Ccnb1	304	RRASKAGEVDVEQHTLAK	321
Rattus norvegicus	Ccnb1	297	RRASKAGEVDVEQHTLAK	314
Gallus gallus	Ccnb2	266	RRASKAGEADAEQHTLAK	283
Drosophila melanogaster	CycB	390	RRYSKAAGAEDEHHTMSK	407
Danio rerio	Ccnb1	273	RRASKIGDVTAEHHTLAK	290
Xenopus tropicalis	Ccnb1	273	RRFAKCAHATMETLTLAR	290
Caenorhabditis elegans	Ccnb3	250	RRFGRVCRVDMKTLTMGR	267

B

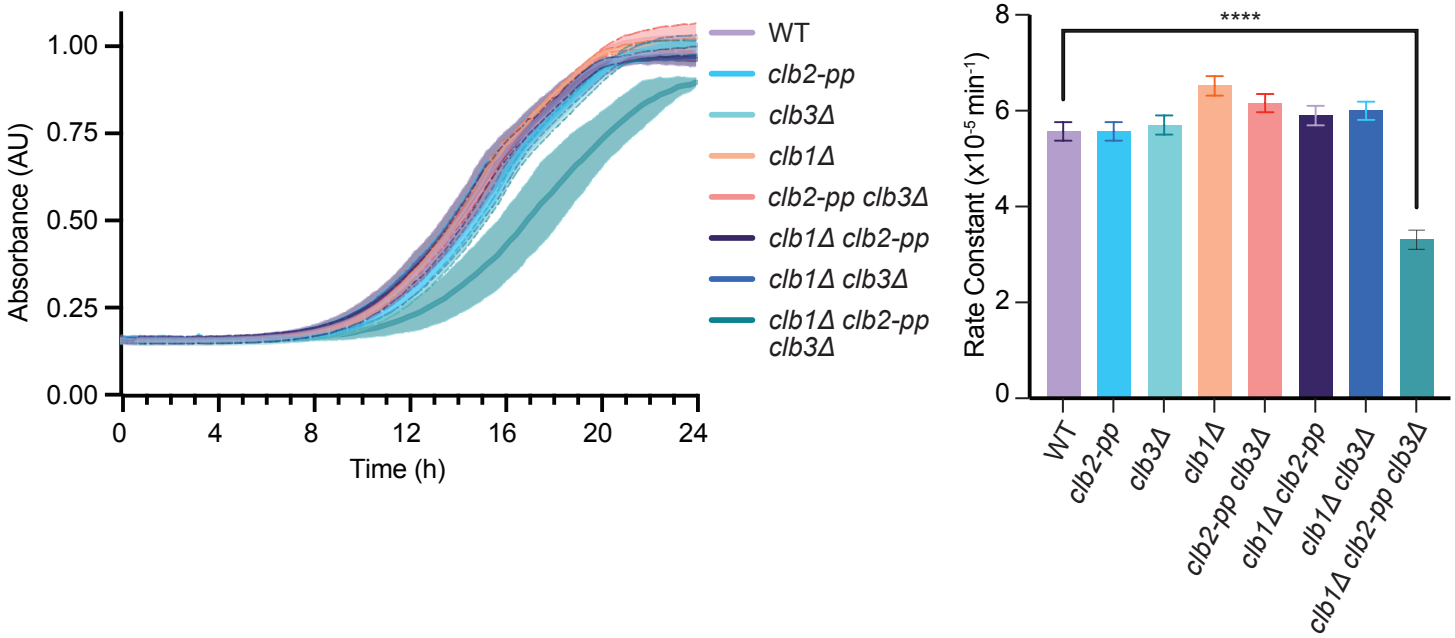

C

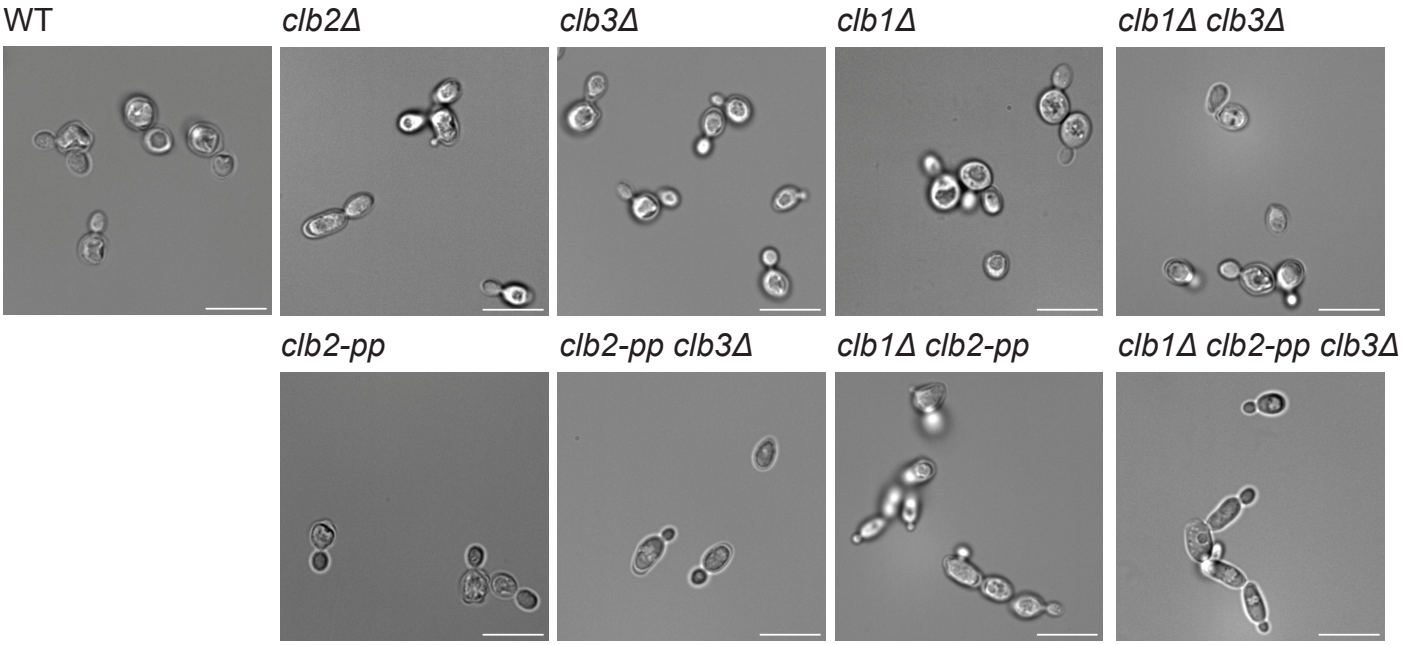

Figure 2

A

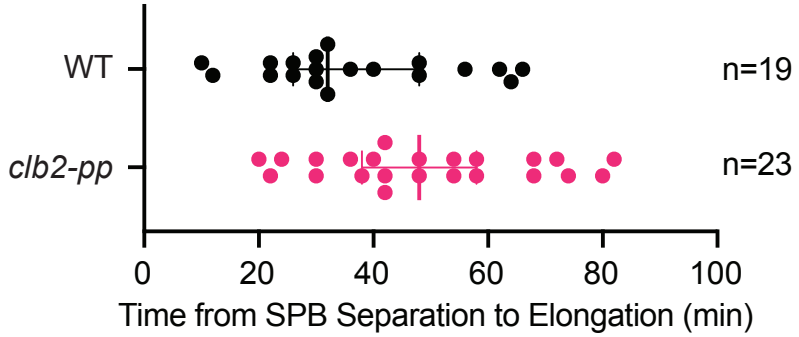

B

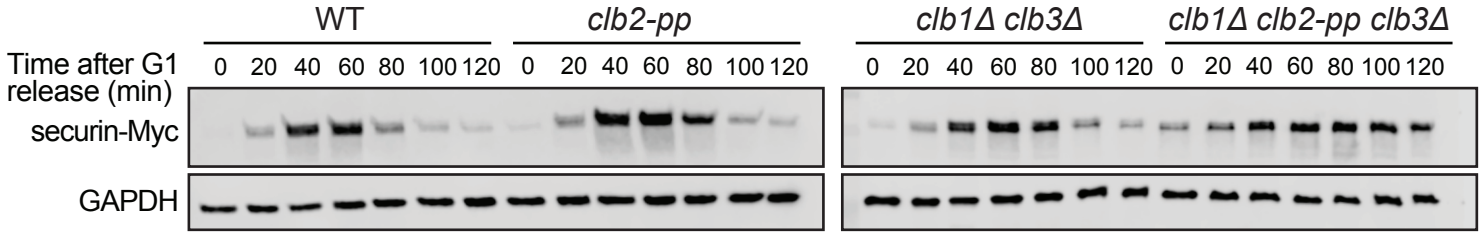

C

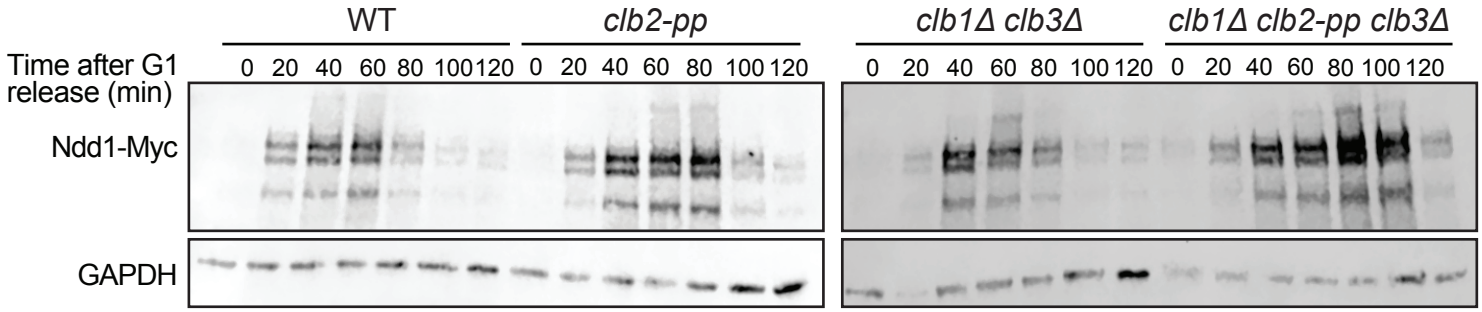

D

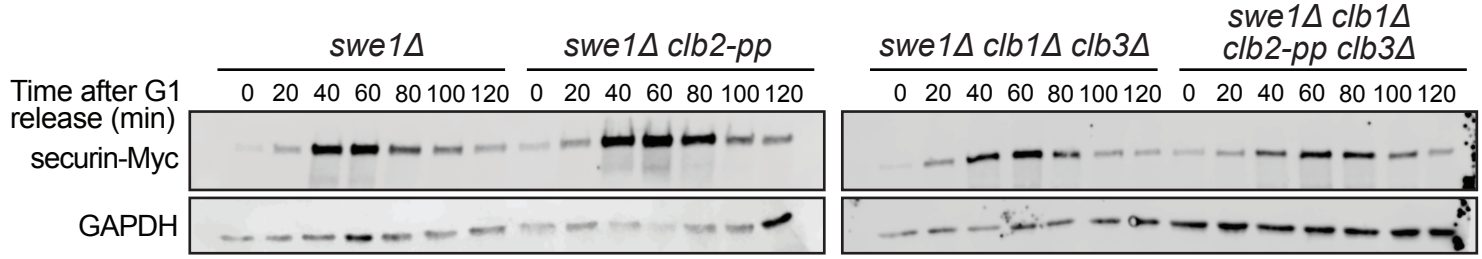

E

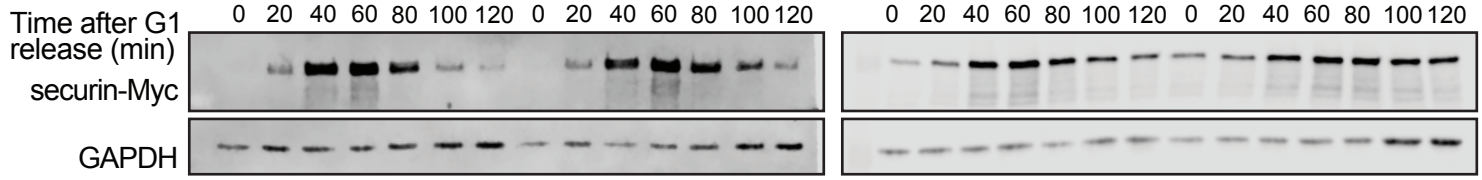

F

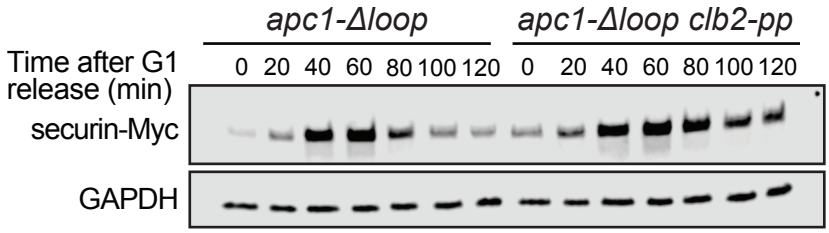

Figure 3

A

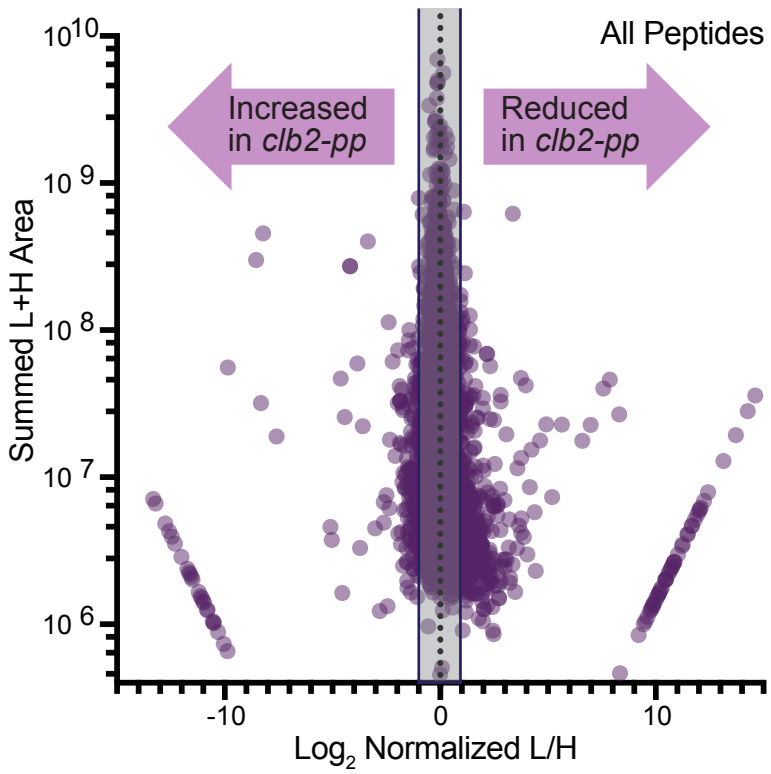
All Peptides
Increased in *clb2-pp*
Reduced in *clb2-pp*
Summed L+H Area
10^{10}
10^{9}
10^{8}
10^{7}
10^{6}
-10
0
10
Log_2 Normalized L/H

B

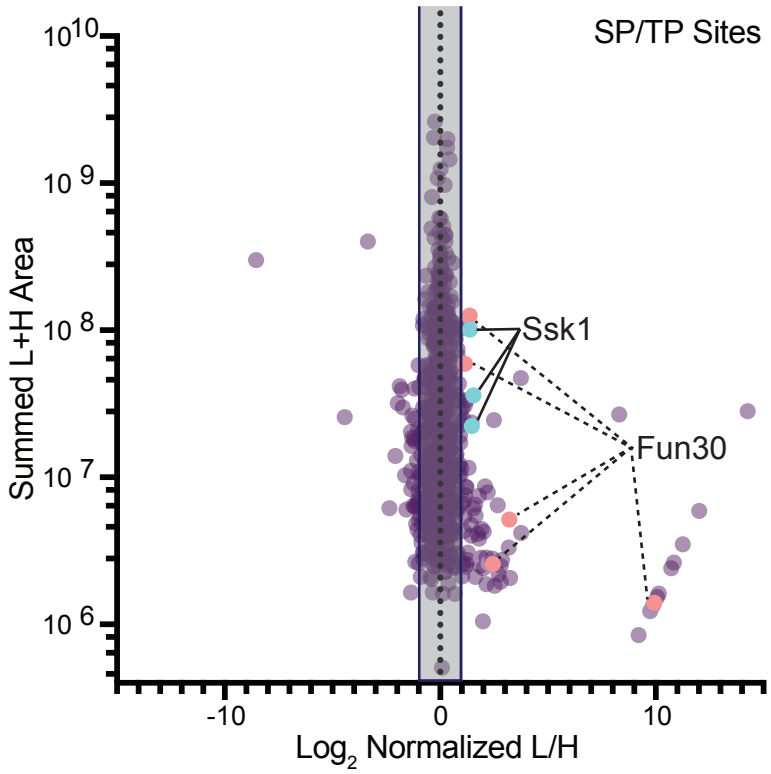
SP/TP Sites
Ssk1
Fun30
Summed L+H Area
10^{10}
10^{9}
10^{8}
10^{7}
10^{6}
-10
0
10
Log_2 Normalized L/H

Figure 4

A

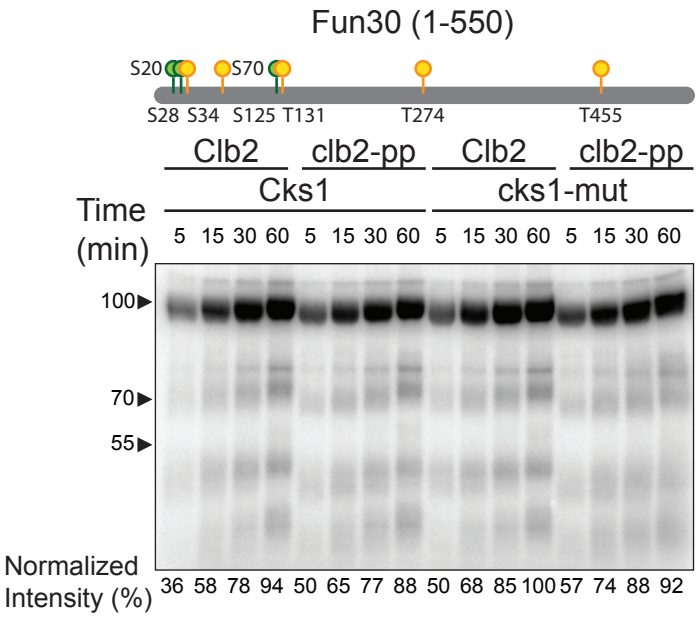
Fun30 (1-550)
S20
S70
S28 S34 S125 T131
T274
T455
Clb2 clb2-pp Clb2 clb2-pp
Cks1 cks1-mut
Time (min)
5 15 30 60 5 15 30 60 5 15 30 60 5 15 30 60
100
70
55
Normalized Intensity (%)
36 58 78 94 50 65 77 88 50 68 85 100 57 74 88 92

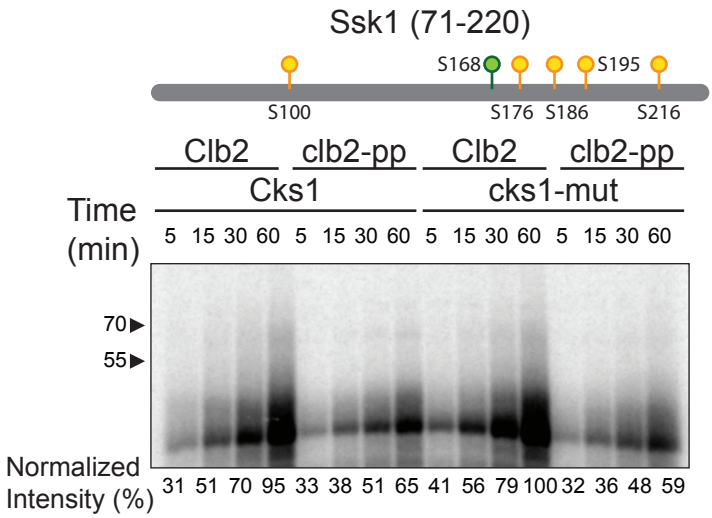
Ssk1 (71-220)
S168
S195
S100
S176 S186
S216
Clb2 clb2-pp Clb2 clb2-pp
Cks1 cks1-mut
Time (min)
5 15 30 60 5 15 30 60 5 15 30 60 5 15 30 60
70
55
Normalized Intensity (%)
31 51 70 95 33 38 51 65 41 56 79 100 32 36 48 59

B

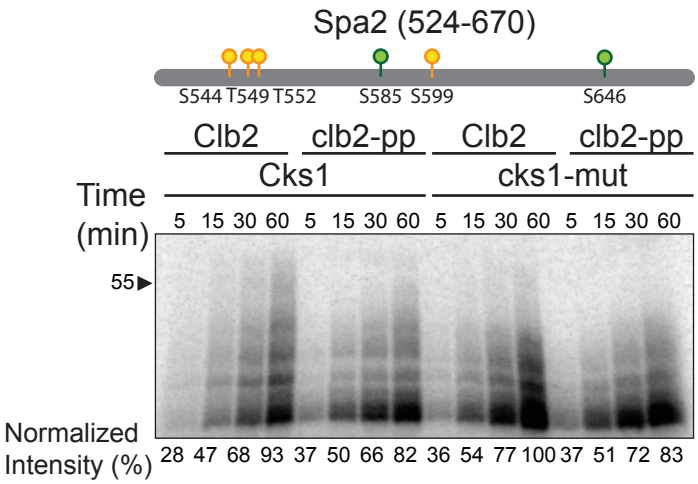
Spa2 (524-670)
S544 T549 T552
S585 S599
S646
Clb2 clb2-pp Clb2 clb2-pp
Cks1 cks1-mut
Time (min)
5 15 30 60 5 15 30 60 5 15 30 60 5 15 30 60
55
Normalized Intensity (%)
28 47 68 93 37 50 66 82 36 54 77 100 37 51 72 83

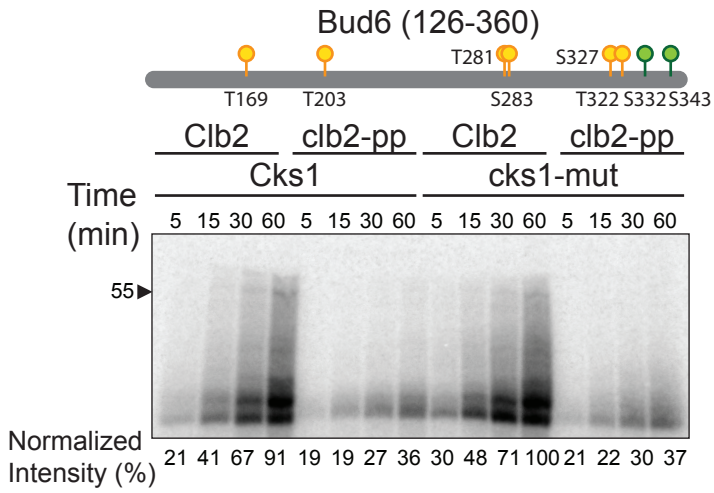
Bud6 (126-360)
T281
S327
T169
T203
S283
T322 S332 S343
Clb2 clb2-pp Clb2 clb2-pp
Cks1 cks1-mut
Time (min)
5 15 30 60 5 15 30 60 5 15 30 60 5 15 30 60
55
Normalized Intensity (%)
21 41 67 91 19 19 27 36 30 48 71 100 21 22 30 37

C

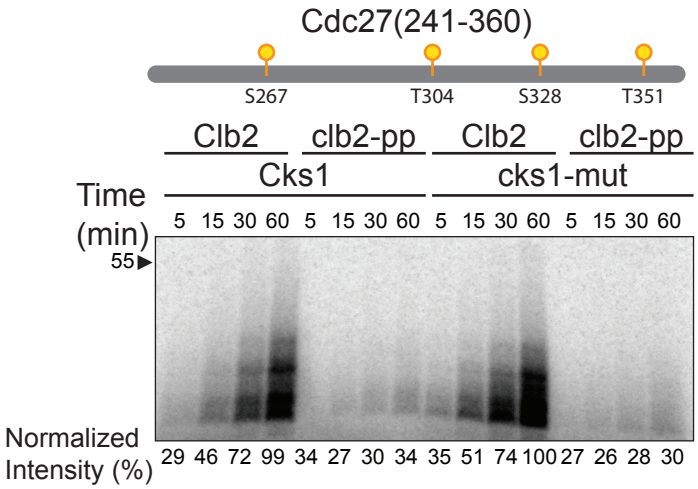
Cdc27(241-360)
S267
T304
S328
T351
Clb2 clb2-pp Clb2 clb2-pp
Cks1 cks1-mut
Time (min)
5 15 30 60 5 15 30 60 5 15 30 60 5 15 30 60
55
Normalized Intensity (%)
29 46 72 99 34 27 30 34 35 51 74 100 27 26 28 30

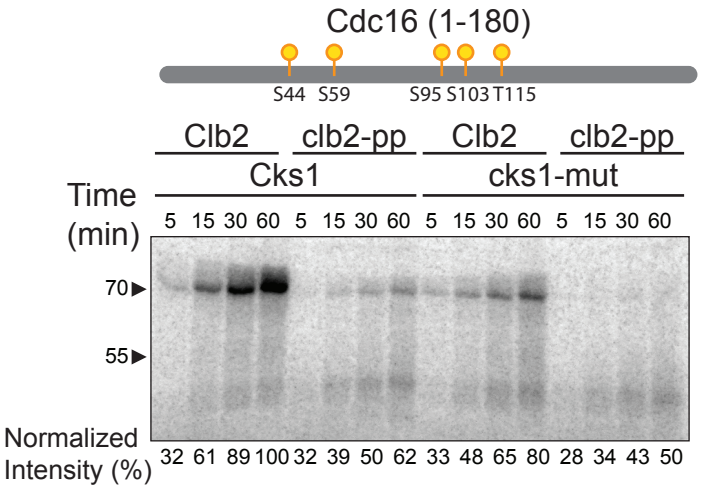
Cdc16 (1-180)
S44 S59
S95 S103 T115
Clb2 clb2-pp Clb2 clb2-pp
Cks1 cks1-mut
Time (min)
5 15 30 60 5 15 30 60 5 15 30 60 5 15 30 60
70
55
Normalized Intensity (%)
32 61 89 100 32 39 50 62 33 48 65 80 28 34 43 50

Supplemental Information

Phosphate-binding pocket on cyclin B governs CDK substrate phosphorylation and mitotic timing

Henry Y. Ng, Armin N. Adly, Devon H. Whelpley, Raymond T. Suhandynata, Huilin Zhou, David O. Morgan

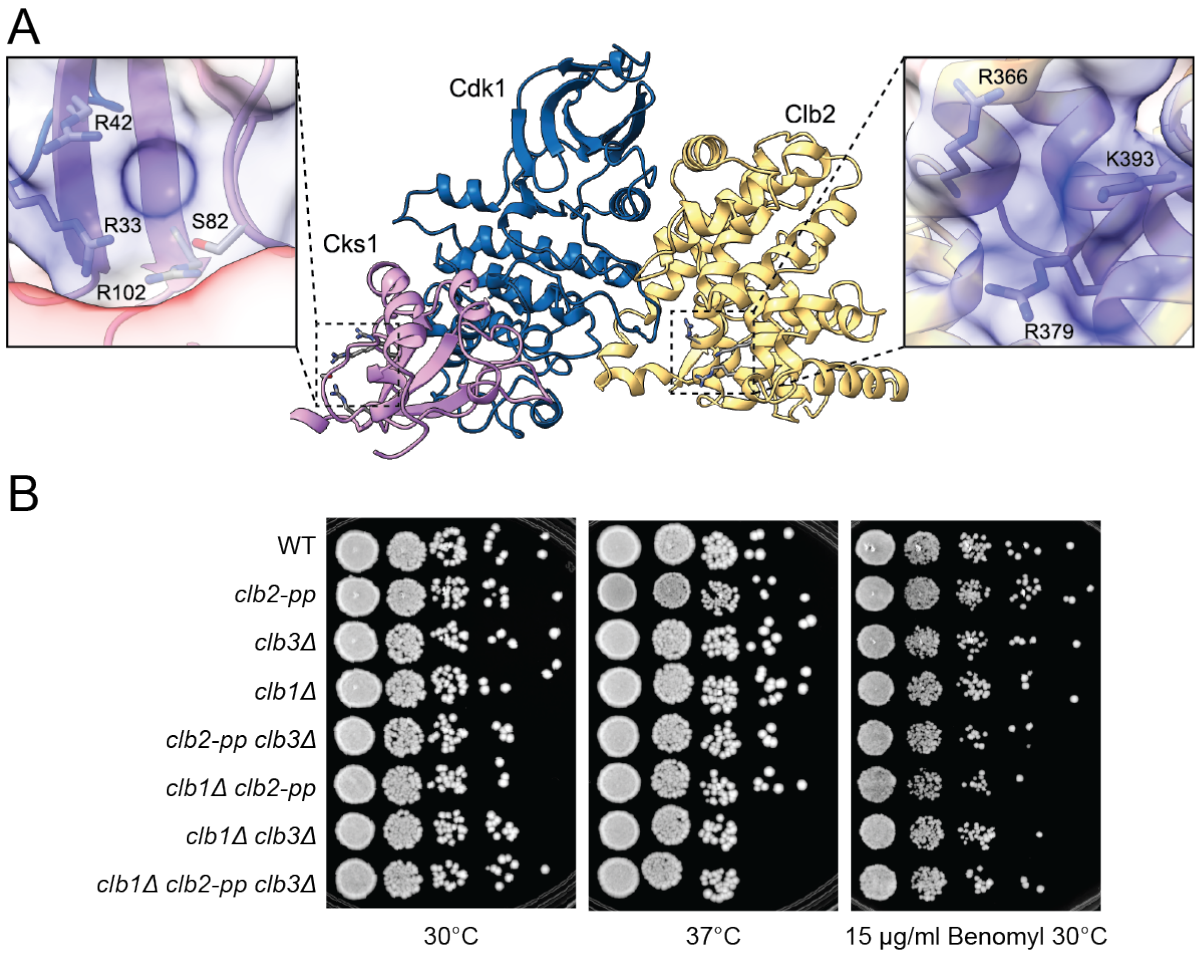

Figure S1. Mutation of the conserved phosphate-binding pocket in Clb2 has little effect on yeast colony growth on plates

A. Alphafold structure model of yeast Cdk1-Clb2-Cks1 complex. Insets show electrostatic surfaces of phosphate-binding pockets in Cks1 (left) and Clb2 (right), colored blue to indicate positive charge.

B. The indicated yeast strains (with endogenous Myc-tagged securin) were spotted on YPD plates and incubated for 48 h at the indicated temperatures. Right panel shows growth on plates containing benomyl (15 µg/ml). Each spot represents 5 µl of a yeast culture at OD_{600}=0.1 followed by four 1:10 serial dilutions.

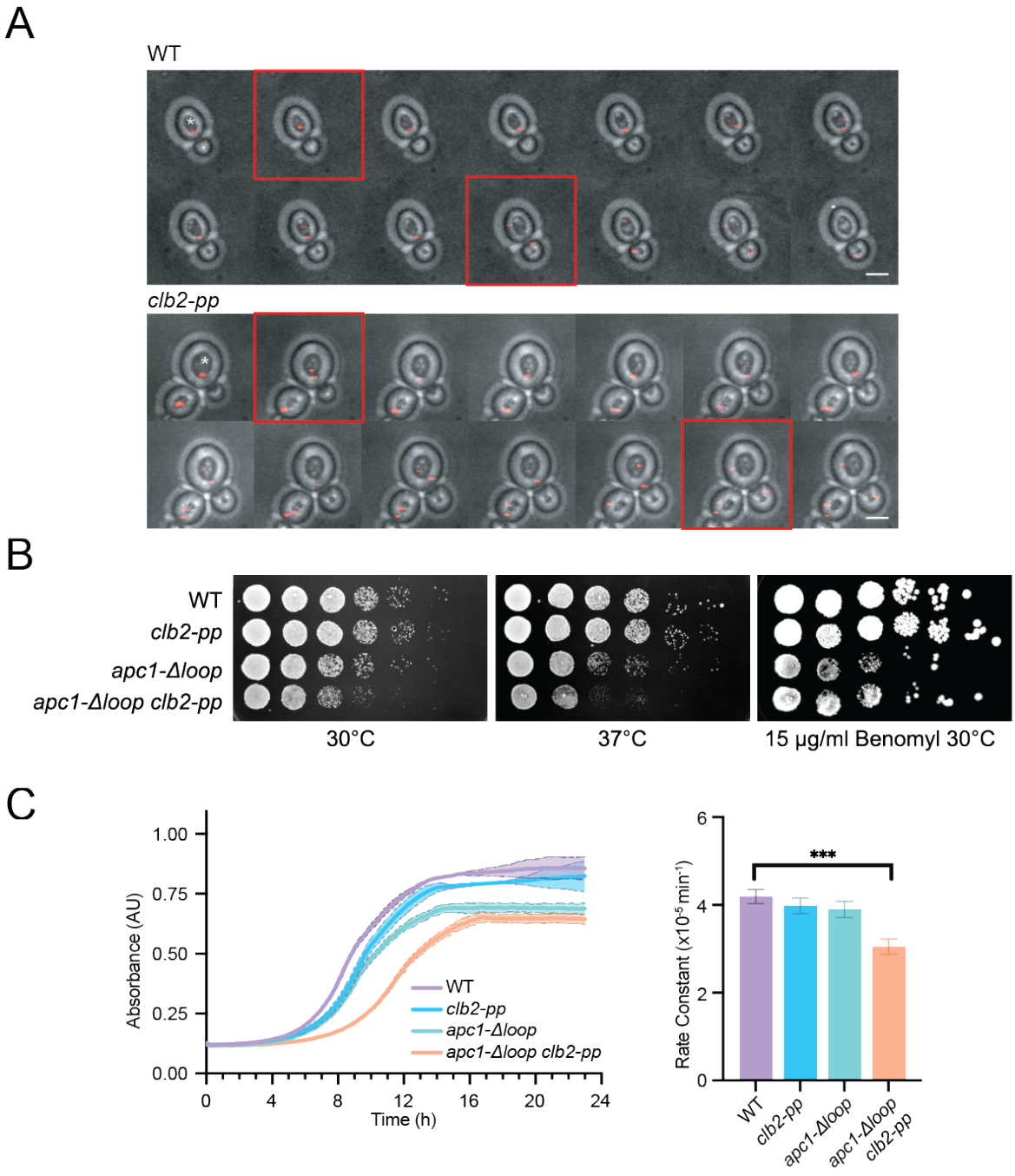

Figure S2. The *clb2-pp* mutation causes single-cell mitotic delay independent of putative regulatory loop in Apc1.

A. Representative fluorescence image montages of yeast strains carrying mCherry-labeled Spc42, captured over 48 min at 2 min intervals. Images depict representative yeast cells with distinct mCherry foci (red). Frames indicated with red outlines depict (1) SPB separation and (2) initiation

of spindle elongation. White asterisks mark the cells entering mitosis used for quantification. The scale bar represents 3 μm. Data from multiple cells in Figure 2A.

B. The indicated yeast strains were spotted on YPD plates and incubated for 48 h at the indicated temperatures. Right panel shows growth on plates containing benomyl (15 μg/ml). Each spot represents 5 μl of a yeast culture at OD_{600}=0.1 followed by four 1:10 serial dilutions.

C. (left) Growth curves of indicated yeast strains, with OD_{600} recorded every 15 min. Data represent mean ± SD of three independent biological replicates. (right) Growth rates calculated by fitting OD_{600}/min to a logistic growth model. Data represent mean ± SD of three independent biological replicates. Statistical significance was determined using ANOVA (***$p < 0.001$).

Fun30

```
   1 MSGSHSNDED DVVQVPETSS PTKVASSSPL KPTSPTVPDA SVASLRSRFT FKPSDPSEGA
  61 HTSKPLPSGS PEVALVNLAR EFPDFSQTLV QAVFKSNSFN LQSARERLTR LRQQRQNWTW
 121 NKNASPKKSE TPPPVKKSLP LANTGRLSSI HGNINNKSSK ITVAKQKTSI FDRYSNVINQ
 181 KQYTFELPTN LNIDSEALSK LPVNYNKKRR LVRADQHPIG KSYESSATQL GSAREKLLAN
 241 RKYGRHANDN DEEEEESMMT DDDDASGDDY TESTPQINLD EQVLQFINDS DIVDLSDLSD
 301 TTMHKAQLIA SHRPYSSLNA FVNTNFNDKD TEENASNKRK RRAAASANES ERLLDKITQS
 361 IRGYNAIESV IKKCSSYGDL VTSQMKKWGV QVEGDNSELD LMNLGEDDDD DNDDGNNDNN
 421 NSNNNNTAGA DATSKEKEDT KAVVEGFDET SAEPTPAPAP APVERETKRI RNTTKPKVVE
 481 DEDDDVDLEA IDDELPQSEH EDDDYEEEDE DYNDEEEDVE YDDGDDDDDD DDEFVATRKN
 541 THVISTTSRN GRKPIVKFFK GKPRLLSPEI SLKDYQQTGI NWLNLLYQNK MSCILADDMG
 601 LGKTCQVISF FAYLKQINEP GPHLVVVPSS TLENWLREFQ KFAPALKIEP YYGSLQEREE
 661 LRDILERNAG KYDVIVTTYN LAAGNKYDVS FLKNRNFNVV VYDEGHMLKN STSERFAKLM
 721 KIRANFRLLL TGTPLQNNLK ELMSLLEFIM PNLFISKKES FDAIFKQRAK TTDDNKNHNP
 781 LLAQEAITRA KTMMKPFILR RRKDQVLKHL PPKHTHIQYC ELNAIQKKIY DKEIQIVLEH
 841 KRMIKDGELP KDAKEKSKLQ SSSSKNLIMA LRKASLHPLL FRNIYNDKII TKMSDAILDE
 901 PAYAENGNKE YIKEDMSYMT DFELHKLCCN FPNTLSKYQL HNDEWMQSGK IDALKKLLKT
 961 IIVDKQEKVL IFSLFTQVLD ILEMVLSTLD YKFLRLDGST QVNDRQLLID KFYEDKDIPI
1021 FILSTKAGGF GINLVCANNV IIFDQSFNPH DDRQAADRAH RVGQTKEVNI TTLITKDSIE
1081 EKIHQLAKNK LALDSYISED KKSQDVLESK VSDMLEDIIY DENSKPKGTK E*
```

Spa2

```
   1 MGTSSEVSLA HHRDIFHYYV SLKTFFEVTG ENRDRSNSTR AQKARAKLLK LSSSQFYELS
  61 TDVSDELQRR IGEDANQPDY LLPKANFHMK RNQARQKLAN LSQTRFNDLL DDILFEIKRR
 121 GFDKDLDAPR PPLPQPMKQE VSKDSDDTAR TSTNSSSVTQ VAPNVSVQPS LVIPKMASID
 181 WSSEEEEEEQ VKEKPNEPEG KQTSMDEKKE AKPALNPIVT DSDLPDSQVL ARDITSMART
 241 PTTTHKNYWD VNDSPIIKVD KDIDNEKGPE QLKSPEVQRA ENNNPNSEME DKVKELTDLN
 301 SDLHLQIEDL NAKLASLTSE KEKEKKEEKE EKEKEKNLKI NYTIDESFQK ELLSLNSQIG
 361 ELSIENENLK QKISEFELHQ KKNDNHNDLK ITDGFISKYS SADGLIPAQY ILNANNLIIQ
 421 FTTRLSAVPI GDSTAISHQI GEELFQILSQ LSNLISQLLL SADLLQYKDQ VILLKASLSH
 481 AITSIRYFSV YGPVLIPKIT VQAAVSEVCF AMCNLIDSAK IKSDSNGEST TSNEGNRQVL
 541 EYSSPTATTP MTPTFPSTSG INMKKGFINP RKPASFLNDV EEEESPVKPL KITQKAINSP
 601 IIRPSSSNGV PTTSRKPSGT GLFSLMIDSS IAKNSSHKED NDKYVSPIKA VTSASNSASS
 661 NISEIPKLTL PPQAKIGTVI PPSENQVPNI KIENTEEDNK RSDITNEISV KPTSSIADKL
 721 KQFEQSSEKK SSPKENPIAK EEMDSKPKLS NKFITSMNDV STDDSSSDGN ENDDADDDDD
 781 FTYMALKQTM KREGSKIEKN NDSKLPANIV ELDLHESPES VKIESPESIK EITSSEMSSE
 841 MPSSSLPKRL VEDVEPSEMP EKGASVESVR KKNFQEPLGN VESPDMTQKV KSLGMTGKAV
 901 GPESDSRVES PGMTGQIKSL NMAGKVVGPE ADSRVESPGM KEQIKSLGMT GKITAQESIK
 961 SPEAARKLAS SGEVDKIESP RMVRESESLE AVGNTIPSNM TVKMESPNLK GNTVSEPQEI
1021 RRDIASSEPI ENVDPPKVLK KIVFPKAVNR TGSPKSVEKT PSSATLKKSG LPEPNSQIVS
1081 PELAKNSPLA PIKKNVELRE TNKPHTETIT SVEPTNKDAN TSWRDADLNR TIKREEEDED
1141 FDRVNHNIQI TGAYTKTGKI DYHKIPVDRK AKSEAEVHTS EEDIDESNNV NGKRADAQIH
1201 ITERKHAFVN PTENSQVKKT SHSPFLNSKP VQYENSESNG GINNHIKIKN TGETTAHDEK
1261 HYSDDDDSSY QFVPMKHEEQ EQEQNRSEEE ESEDDDEEEE DSDFDVDTFD IENPDNTLSE
1321 LLLYLEHQTM DVISTIQSLL TSIKKPQVTK GNLRGESNAI NQVIGQMVDA TSISMEQSRN
1381 ANLKKHGDWV VQSLRDCSRR MTILCQLTGD GILAKEKSDQ DYADKNFKQR LAGIAFDVAK
1441 CTKELVKTVE EASLKDEINY LNSKLK*
```

hAPC3

```
   1 MTVLQEPVQA AIWQALNHYA YRDAVFLAER LYAEVHSEEA LFLLATCYYR SGKAYKAYRL
  61 LKGHSCTTPQ CKYLLAKCCV DLSKLAEGEQ ILSGGVFNKQ KSHDDIVTEF GDSACFTLSL
 121 LGHVYCKTDR LAKGSECYQK SLSLNPFLWS PFESLCEIGE KPDPDQTFKF TSLQNFSNCL
 181 PNSCTTQVPN HSLSHRQPET VLTETPQDTI ELNRLNLESS NSKYSLNTDS SVSYIDSAVI
 241 SPDTVPLGTG TSILSKQVQN KPKTGRSLLG GPAALSPLTP SFGILPLETP SPGDGSYLQN
 301 YTNTPPVIDV PSTGAPSKKS VARIGQTGTK SVFSQSGNSR EVTPILAQTQ SSGPQTSTTP
 361 QVLSPTITSP PNALPRRSSR LFTSDSSTTK ENSKKLKMKF PPKIPNRKTK SKTNKGGITQ
 421 PNINDSLEIT KLDSSIISEG KISTITPQIQ AFNLQKAAAE GLMSLLREMG KGYLALCSYN
 481 CKEAINILSH LPSHHYNTGW VLCQIGRAYF ELSEYMQAER IFSEVRRIEN YRVEGMEIYS
 541 TTLWHLQKDV ALSVLSKDLT DMDKNSPEAW CAAGNCFSLQ REHDIAIKFF QRAIQVDPNY
 601 AYAYTLLGHE FVLTEELDKA LACFRNAIRV NPRHYNAWYG LGMIYYKQEK FSLAEMHFQK
 661 ALDINPQSSV LLCHIGVVQH ALKKSEKALD TLNKAIVIDP KNPLCKFHRA SVLFANEKYK
 721 SALQELEELK QIVPKESLVY FLIGKVYKKL GQTHLALMNF SWAMDLDPKG ANNQIKEAID
 781 KRYLPDDEEP ITQEEQIMGT DESQESSMTD ADDTQLHAAE SDEF*
```

Ssk1

```
  1 MLNSALLWKV WLRIDNSTDE VNQPIAVQFD EIDTVDDLKS RFFQKLSSTR WREINDNASI
 61 AIGLYAPKFD NQADNTSSNN TNDNSCRSKS NGAGSGANLS VNSNTKSSVS PTAGSFGLSK
121 DLAKDRNVLQ HPKPTQKRGA LYDAFAAVPT VAATTNVDFP PNEAPMLSPQ RPYSTSPKQF
181 PATTKSPLLR FASVSPYPKF HSDNQIMASA GLTYVSPHNK NKYTRPLIRK GLNFTTESVN
241 DCTYKIIFEP DELAINIYKE LFGTMGSQPA SQPLLIFSNV NLRQDVPPLD ILNVVDYVPT
301 NEEISQQKTQ PTDHGAVGVF HLDDHISPGE QGLKQTIGDK ADLKGKDGNS SPQEFKLITD
361 EEQLRRASQE LKDEEKDAES PWQAILLLPK GYKGGVDFRN KPVAHTDSSF NNEDTITHSE
421 LEVNTGSPSQ ESGSLNEAGI GITQPMSEVQ RRKEDVTPAS PILTSSQTPH YSNSLYNAPF
481 AVSSPPDPLP NLFTTTSEKV FPKINVLIVE DNVINQAILG SFLRKHKISY KLAKNGQEAV
541 NIWKEGGLHL IFMDLQLPVL SGIEAAKQIR DFEKQNGIGI QKSLNNSHSN LEKGTSKRFS
601 QAPVIIVALT ASNSQMDKRK ALLSGCNDYL TKPVNLHWLS KKITEWGCMQ ALIDFDSWKQ
661 GESRMTDSVL VKSPQKPIAP SNPHSFKQAT SMTPTHSPVR KNSNLSPTQI EL*
```

Bud6

```
  1 MKMAVDDPTY GTPKIKRTAS SSSSIETTVT KLLMSTKHLL QVLTQWSKGT TSGRLVSDAY
 61 VQLGNDFKVV SKFFMHAKVD MSDVGDVPMA LRRVLEVTLR EPPSDETLNK HLPKIREIIV
121 TLLDKLKVKQ AILKNMQQEH RISVKSHHQQ NPSFTSNLSL GSEGTREGTP LSSRKSSIVR
181 DQRQSDSVEN SYGEKVNSTS TGTPSAQSAE ATLTKPRTNI KQNLKSNNAP NASDDDDALS
241 QLKKGTNLQR RASKRYSAYH MAKLTNQSTT EAAAAAGLMT TPSPSMLHLE ETVRKSKLYG
301 NNNNDDDRNI NSAENKGKSI DDVSKASPLA KTPLPIENVR ASPRRLSSVV TTSPDKAMNG
361 TCPVFLRIGD KTKKCHVQLP TTKNALRLLF IERFAYSPGA NSFPDIYIMD PQYGVFYELE
421 ELNLLDIKEG FVIELKLEEN PNNTIKEFID TVKMEISNSQ NDIIRHLKEM SFGSAISGKQ
481 TEVLPQPGLE ANKHDLVGQN KKDDDKTIKD IQYELGKIKQ VHNINRSNIN ETIFNILRKV
541 DNFKSLSFSA KNSSNRMYME KSQTELGDLS DTLLSKVDDL QDVIEIMRKD VAERRSQPAK
601 KKLETVSKDL ENAQADVLKL QEFIDTEKPH WKKTWEAELD KVCEEQQFLT LQEELILDLK
661 EDLGKALETF DLIKLCCEEQ EKNPSRSKSN PILPIMRPGT FNQVREQVMV AVQSLNPDHD
721 SRVEAIDKAE KMWEMERKLK ASNEFDDELE NFVGNSNLKK SGGFEEVERI RKQKDEANLR
781 AYFGPGFT*
```

Cdc16

```
  1 MKFCLYCCHC YIVICGKATH YYKSSKATSN LKSSNRVLMR NPMSPSEQHS QHNSTLAASP
 61 FVSNVSAART QQSLPTDAQN DRLQQPWNRT NTATSPYQSL ANSPLIQKLQ ANIMTPHQPS
121 ANSNSNSNSI TGNVVNDNNL LASMSKNSMF GSTIPSTLRK VSLQREYKDS VDGVVRDEDN
181 DEDVHNNGDA AANANNDRES KLGHNGPLTT TTLTTTTTAT QLDVSELSAI ERLRLWRFDA
241 LMQHMYRTAE YIADKVYNIS NDPDDAFWLG QVYYNNNQYV RAVELITRNN LDGVNILCRY
301 LLGLSFVKLQ RFDDALDVIG EYNPFSEDPS TTAANTMSNN GNNSNTSQPV TDGGIKMESS
361 LCFLRGKIYF AQNNFNKARD AFREAILVDI KNFEAFEMLL SKNLLTPQEE WDLFDSLDFK
421 EFGEDKEIMK NLYKINLSKY INTEDITKSN EILAKDYKLA DNVDVVRSKV DICYTQCKFN
481 ECLELCETVL ENDEFNTNIL PAYIGCLYEL SNKNKLFLLS HRLAETFPKS AITWFSVATY
541 YMSLDRISEA QKYYSKSSIL DPSFAAAWLG FAHTYALEGE QDQALTAYST ASRFFPGMHL
601 PKLFLGMQFM AMNSLNLAES YFVLAYDICP NDPLVLNEMG VMYFKKNEFV KAKKYLKKAL
661 EVVKDLDPSS RTTISIQLNL GHTYRKLNEN EIAIKCFRCV LEKNDKNSEI HCSLGYLYLK
721 TKKLQKAIDH LHKSLYLKPN NSSATALLKN ALELNVTLSL DASHPLIDKS NLMSQASKDK
781 ASLNKKRSSL TYDPVNMAKR LRTQKEIFDQ NNKALRKGGH DSKTGSNNAD DDFDADMELE
841 *
```

Cdc27

```
  1 MAVNPELAPF TLSRGIPSFD DQALSTIIQL QDCIQQAIQQ LNYSTAEFLA ELLYAECSIL
 61 DKSSVYWSDA VYLYALSLFL NKSYHTAFQI SKEFKEYHLG IAYIFGRCAL QLSQGVNEAI
121 LTLLSIINVF SSNSSNTRIN MVLNSNLVHI PDLATLNCLL GNLYMKLDHS KEGAFYHSEA
181 LAINPYLWES YEAICKMRAT VDLKRVFFDI AGKKSNSHNN NAASSFPSTS LSHFEPRSQP
241 SLYSKTNKNG NNNINNNVNT LFQSSNSPPS TSASSFSSIQ HFSRSQQQQA NTSIRTCQNK
301 NTQTPKNPAI NSKTSSALPN NISMNLVSPS SKQPTISSLA KVYNRNKLLT TPPSKLLNND
361 RNHQNNNNNN NNNNNNNNNN NNNNNNNNII NKTTFKTPRN LYSSTGRLTT SKKNPRSLII
421 SNSILTSDYS ITLPEIMYNF ALILRSSSQY NSFKAIRLFE SQIPSHIKDT MPWCLVQLGK
481 LHFEIINYDM SLKYFNRLKD LQPARVKDME IFSTLLWHLH DKVKSSNLAN GLMDTMPNKP
541 ETWCCIGNLL SLQKDHDAAI KAFEKATQLD PNFAYAYTLQ GHEHSSNDSS DSAKTCYRKA
601 LACDPQHYNA YYGLGTSAMK LGQYEEALLY FEKARSINPV NVVLICCCGG SLEKLGYKEK
661 ALQYYELACH LQPTSSLSKY KMGQLLYSMT RYNVALQTFE ELVKLVPDDA TAHYLLGQTY
721 RIVGRKKDAI KELTVAMNLD PKGNQVIIDE LQKCHMQE*
```

Figure S3. Amino acid sequences of the CDK substrates analyzed in this study.

For Fun30 and Ssk1, the peptide sequence identified in the MS analysis (Table S2) is underlined. CDK consensus sequences (S/T*-P) are highlighted in orange, and S/T residues identified previously as phosphorylation sites *in vivo* are shown in bold. Highlighted in blue is the disordered fragment used for kinase reactions in Figures 4, S4A, S5, S6.

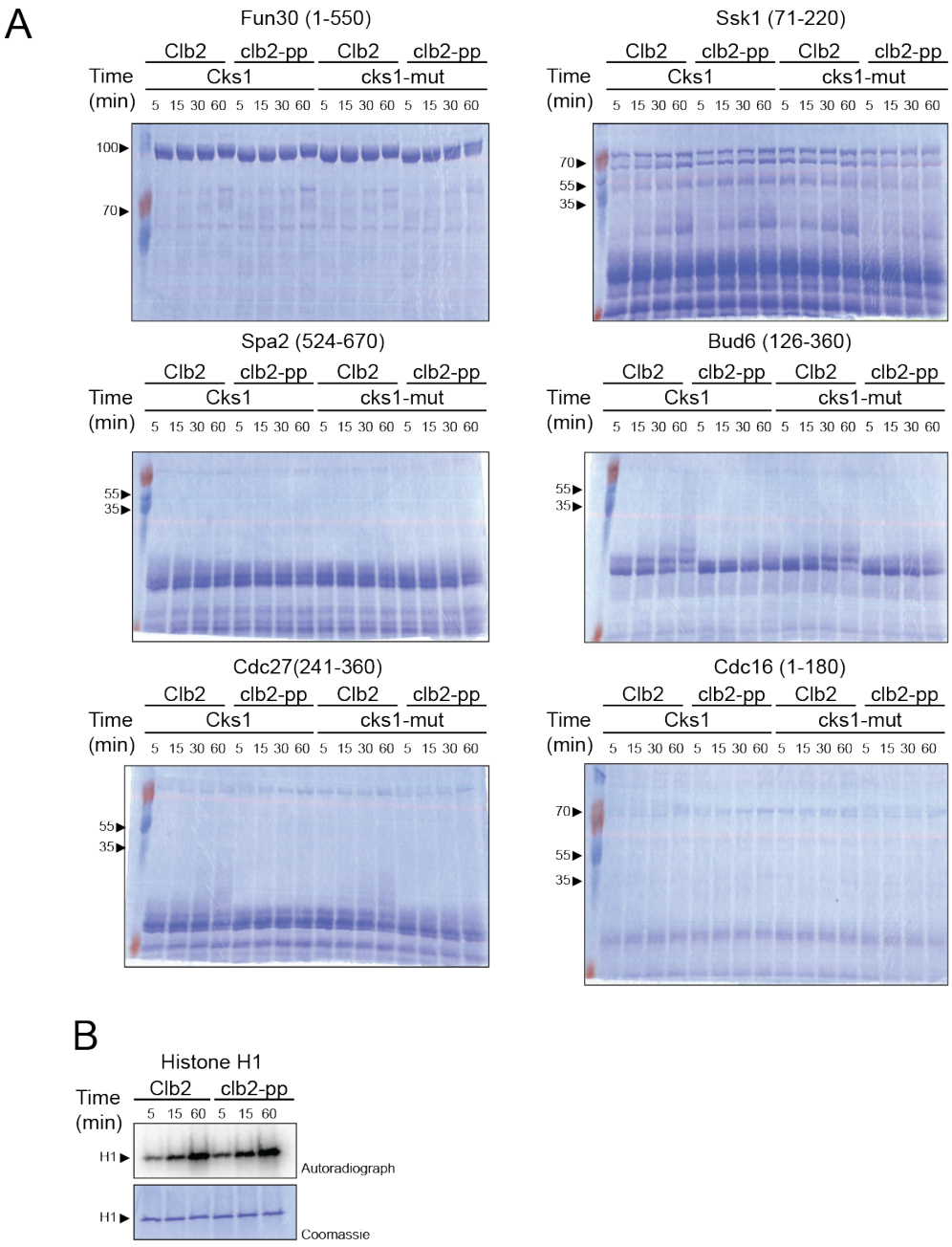

Figure S4. Phospho-pocket mutations reduce phosphorylation of multiple CDK substrates *in vitro*.

A. Phos-tag polyacrylamide gels for the kinase assays in Figure 4 were stained with Coomassie Brilliant Blue to demonstrate extensive PP-dependent multisite phosphorylation of some substrates.

B. To confirm that equal amounts of wild-type and clb2-pp kinase activities were used in Figure 4, Histone H1.0 (Sigma H1917) was incubated with wild-type or clb2-pp Clb2-Cdk1 and radiolabeled ATP. Reaction products were analyzed by SDS-PAGE and autoradiography.

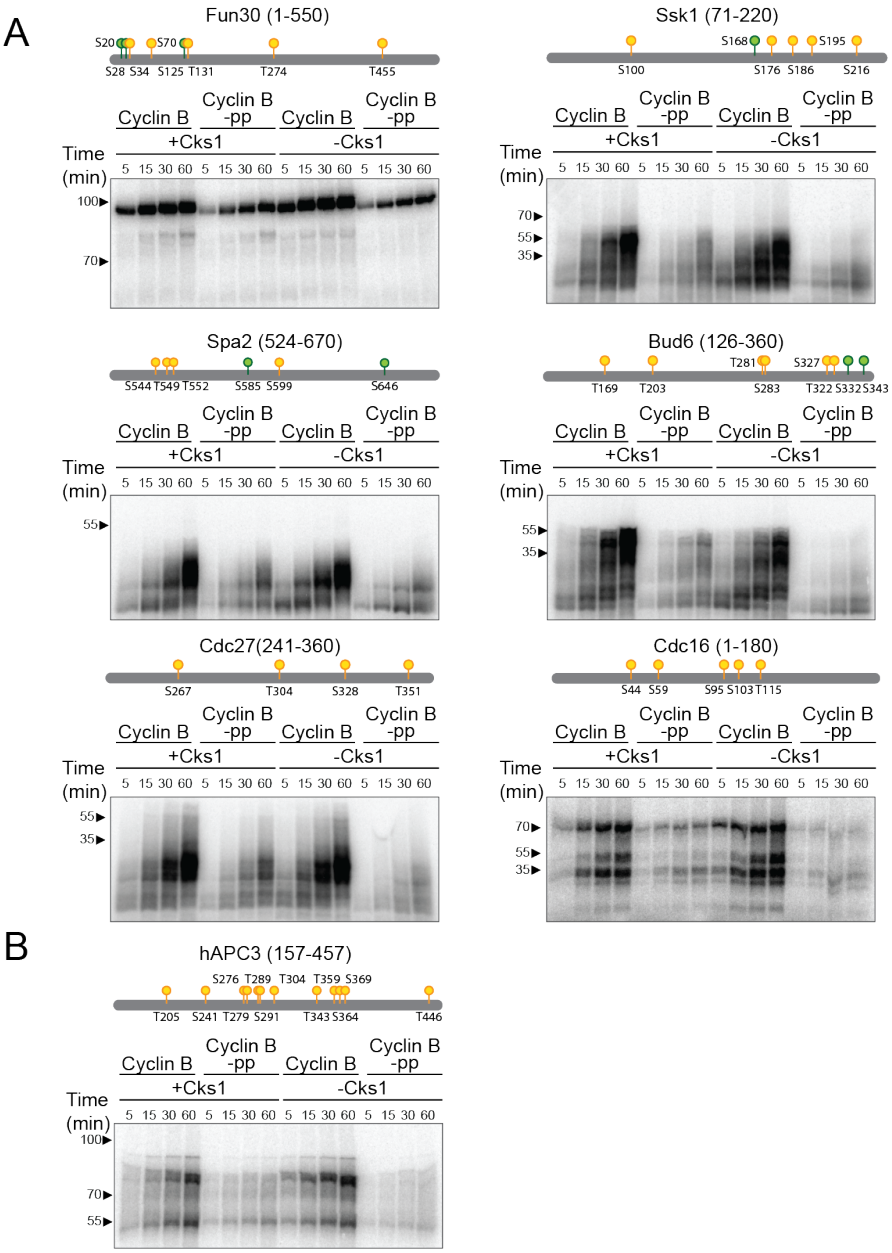

Figure S5. Phospho-pocket mutations reduce phosphorylation by human cyclin B1-Cdk1.

A. The six yeast protein fragments analyzed in Figure 4 were incubated with wild-type or pp-mutant human cyclin B1-Cdk1, with or without human Cks1, plus radiolabeled ATP. Reaction products were analyzed by Phos-tag SDS-PAGE and autoradiography. Diagrams at top indicate optimal (S/T*-P-x-K/R; green) and suboptimal (S/T*-P; yellow) CDK consensus sites in the tested fragment (see Figure S3 for complete sequences). Representative of 2 independent experiments. Coomassie Blue-stained gels in Figure S6.

B. Phosphorylation of human Apc3 (aa 157-457) by human cyclin B1-Cdk1 was analyzed as in panel A. Representative of 2 independent experiments. Coomassie Blue-stained gel in Figure S6.

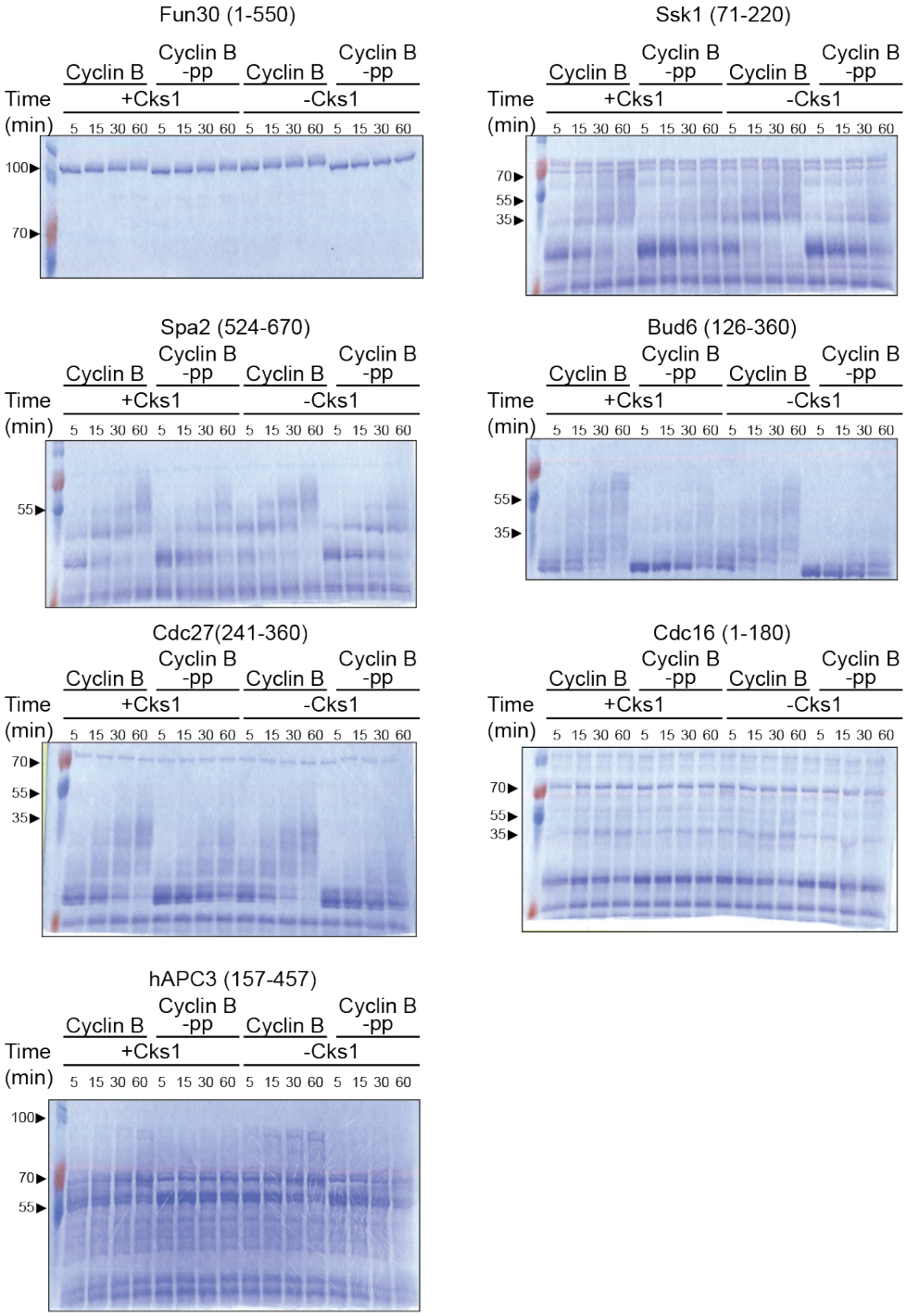

Figure S6. Multisite phosphorylation of CDK substrates by human cyclin B1-Cdk1. Phos-tag polyacrylamide gels for the kinase assays in Figure S5 were stained with Coomassie Brilliant Blue to demonstrate extensive PP-dependent multisite phosphorylation of some substrates.

Table S1. Phosphopeptides identified in SILAC MS analysis.

Attached Excel document (Table S1.xlsx).

Table S2. Phosphopeptides containing a CDK site with Log2 L/H > 1.

		Normalized Log2 of L/H ratio	[S/T]PxK/R sites	[S/T]P sites	Ubersax et al. P-score Table S1*	Holt et al. Table S1**	Peptide sequence
YPL202C	AFT2	10.06	1	5			L.EYKA**S**LNLPLV**T**PII**S**CDCGLTK.E
YOL062C	APM4	1.28	0	5	1.6		R.NMGGLLDSPDGNDVLSS**S**S**S**P**T**SSAGELHFPK.F
YLR399C	BDF1	1.43	0	5			R.DAS**SL**S**P**TSAGSR.K
YLR399C	BDF1	1.54	0	5			R.DAS**SL**S**P**TSAGSr.K
YCL029C	BIK1	2.21	1	3			R.LTNQF**S**PMDDPK**S**P**T**PMR.S
YFL007W	BLM10	1.32	2	6	1.2	X	R.**S**A**T**PTLQDQK.L
YDL099W	BUG1	2.70	0	4		X	K.NSSA**T**GSIG**S**E**T**PDLEGTPGEESTQEETVK.A
YER026C	CHO1	1.27	0	1			R.A**SS**IFSINT**T**PLAPPNATDIQK.F
YER026C	CHO1	1.81	0	1			R.ASSIF**S**IN**TT**PLAPPNATDIQK.F
YOR042W	CUE5	2.67	1	5		X	K.VVAETTYID**T**PDTE**T**KKK.W
YDL117W	CYK3	9.21	1	8	1.6		R.NTNIYS**S**SVSSPK**S**PK.A
YIR023W	DAL81	1.44	2	19	3.7	X	R.SGVQSQIPIQFNVG**S**PAM**T**EQG**S**PLNQWK.N
YPL049C	DIG1	1.13	0	6			K.RVNDSYD**S**PL**S**GTASTGK.T
YKL204W	EAP1	8.31	0	7			R.E**S**A**S**HE**T**PTDLRPVIPR.G
YAL019W	FUN30	1.15	3	10	5.8		K.AVVEGFDE**TS**AEP**T**PAPAPAPVER.E
YAL019W	FUN30	1.37	3	10	5.8		K.AVVEGFDE**TS**AEP**T**PAPAPAPVER.E
YAL019W	FUN30	2.45	3	10	5.8		K.AVVEGFDE**TS**AEP**T**PAPAPAPVER.E
YAL019W	FUN30	3.21	3	10	5.8		K.AVVEGFDE**TS**AEP**T**PAPAPAPVER.E
YAL019W	FUN30	9.88	3	10	5.8		K.AVVEGFDE**TS**AEP**T**PAPAPAPVER.E
YOL051W	GAL11	3.24	1	18		X	K.KL**S**ISNAA**S**QQP**T**PR.S
YEL043W	GTA1	2.42	0	13		X	R.STNESLFSTTG**T**PMSSYK.A
YOR025W	HST3	1.64	1	6	1.8		K.IL**S**PEN**SS**EEDEEENLDTR.K
YOR025W	HST3	2.53	1	6	1.8		K.IL**S**PEN**SS**EEDEEENLDTR.K
YFL013C	IES1	2.14	1	9			K.SGSQEEA**S**P**S**SIQ**S**ETETVTTK.S
YDR229W	IVY1	1.15	1	3			M.PDNNTEQLQG**S**PS**S**DQR.L
YJR091C	JSN1	1.89	2	11	2		K.MMESSIDGVTMDRPG**SL**T**P**PQDMEK.L
YJR091C	JSN1	2.24	2	11	2		K.MMESSIDGVTMDRPG**SL**T**P**PQDMEK.L
YLL019C	KNS1	1.10	1	5			K.AVNLTIAH**ST**S**P**FSNPPAQIASLPQSNLK.K
YLL019C	KNS1	1.14	1	5			K.AVNLTIAH**ST**S**P**FSNPPAQIASLPQSNLK.K
YLL019C	KNS1	1.79	1	5			K.AVNLTIAHS**TS**P**F**SNPPAQIASLPQSNLK.K
YHR082C	KSP1	1.20	0	10			R.RG**S**TTTVQH**S**PGAYIPPNAR.N
YDL240W	LRG1	1.62	1	6			R.SLNTA**S**PM**T**VQVK.N
YER068W	MOT2	3.18	0	11			R.SGIHNNISTSTAGSN**T**NLLSENFTG**T**P**S**PAAMR.A
YMR037C	MSN2	1.11	1	10			R.NTNLNITTNS**T**SS**S**NA**S**PNTTTMNANADSNIAGNPK.N
YKL062W	MSN4	1.06	1	13		X	R.RG**S**TI**S**PTTTINNSNPNFK.L
YKL062W	MSN4	1.16	1	13		X	R.RG**S**TI**S**PTTTINNSNPNFK.L
YKL062W	MSN4	1.64	1	13		X	R.RG**S**TI**S**PTTTINNSNPNFK.L
YKL062W	MSN4	2.08	1	13		X	R.RG**S**TI**S**PTTTINNSNPNFK.L
YMR153W	NUP53	9.75	2	7	1.4		K.TDNIEDPNLSSNITFDGKP**T**A**T**P**S**PFRPLEK.T
YHR118C	ORC6	1.02	4	6	4.1	X	K.QFAW**T**P**S**PK.K
YHR097C	PAL2	1.86	1	4			K.NVDTIDKMDV**T**GLFGG**S**FHHDGPFDAC**T**P.Q
YIR006C	PAN1	3.75	0	14			K.SVTESSPFVP**S**S**T**P**T**PVDDR.S
YNR070W	PDR18	12.02	1	4			Y.WLD**S**PEYARLK.G
YOL011W	PLB3	3.75	0	4			D.L**S**QDFNDIAVY**S**PNPFK.D
YBL035C	POL12	2.49	0	12		X	K.SSDAK**T**PG**S**STFQTPTTNTPTTSR.Q
YER075C	PTP3	9.94	0	11		X	R.NVLSDSPMSS**SS**PISALFK.F
YKR090W	PXL1	1.92	1	9	2.9		K.IPEINVTRE**S**N**T**P**S**LTMNALDSK.L
YPR115W	RGC1	10.72	1	17			R.LSDIVYPNMK**S**PLAK.C
YPL089C	RLM1	10.85	1	12			R.SSKI**S**PL**S**ASASGPL**T**LQK.G
YPL089C	RLM1	11.26	1	12			R.SSKI**S**PLSASA**S**GPL**T**LQK.G
YLR357W	RSC2	1.99	1	10		X	R.**ST**TPSHSG**T**PQPLGPR.H
YPL085W	SEC16	1.00	2	28	1.6	X	K.TSP**S**PTGPNPNNSP**S**PS**S**PISR.L
YPL085W	SEC16	1.02	2	28	1.6	X	K.TSPSP**T**GPNPNNSP**S**PS**S**PISR.L
YDL195W	SEC31	1.23	0	20		X	R.VA**T**PL**S**GGVPPAPLPK.A
YKR072C	SIS2	2.02	1	13		X	R.Q**SI**SPTLSNATTTTTK.S
YNL311C	SKP2	2.81	0	8			R.LNDE**T**PII**TS**ER.L
YNL243W	SLA2	2.15	2	10	1.9	X	K.LITSEDNEN**TS**PEQFIVA**S**K.E
YOR290C	SNF2	2.01	0	14			K.LEGSENSEPPALE**S**SPV**T**GDN**S**PSEDFMDIPKPR.T
YOR290C	SNF2	2.87	0	14			K.LEGSENSEPPALE**S**SPV**T**GDN**S**PSEDFMDIPKPR.T
YLR006C	SSK1	1.38	3	18	2.8	X	R.FA**S**V**S**PYPK.F
YLR006C	SSK1	1.47	3	18	2.8	X	R.FA**S**V**S**PYPK.F
YLR006C	SSK1	1.55	3	18	2.8	X	R.FA**S**V**S**PYPK.F
YDR320C	SWA2	1.75	1	9			R.TAPDVSHS**SS**PTSGILIEENSR.R
YPL105C	SYH1	1.46	0	11			R.ASSLDDFI**S**R**T**P**S**PSSSALNSSNTSNAWTTVSSK.S
YHR009C	TDA3	1.23	0	5			R.**S**HTN**S**ASDLDSV**S**PVEQLR.E
YJL048C	UBX6	2.81	0	3			K.LSSLDMVSDGGGGGGGDSM**TPS**AY**TT**PR.M
YDR213W	UPC2	1.22	1	11			R.NSNI**S**PS**T**PSAVLNDRQEMQDSISSLGNL**T**K.A
YDR485C	VPS72	10.15	1	9			K.QVTFTDHPQVAIID**T**EE**S**PSKK.D
YML076C	WAR1	1.10	0	8		X	R.**S**R**S**P**T**PFESPMVNVSTK.S

This table lists the 69 phosphopeptides with 2-fold or greater enrichment in the wild-type culture, indicating reduced phosphorylation in the *clb2-pp* mutant.

19 peptides were identified multiple times (shaded yellow), so there are 50 unique proteins identified.

Bolded letters in peptide sequence indicate phosphorylated residues.

*Column F indicates proteins identified as Cdk1-Clb2 substrates in a previous screen of 695 candidate proteins; P-score of 2 or greater (pink highlight) indicates a good Cdk1 substrate (ref 1).

**Column G indicate proteins identified in a previous mass spectrometric analysis of phosphopeptides with reduced phosphorylation after acute inhibition of Cdk1 in vivo (ref. 2).

Table S3. Yeast Strains used in this work.

Name	Genotype	Source
DOM123	*W303, MATa, bar1-HisG*	ATCC
JBA53	*trp1::pGAL-NDD1-9xMYC-TRP1*	[7]
HN40	*clb2Δ::HYGR, trp1::pGAL-NDD1-9xMYC-TRP1*	This Study
JBA71	*clb2::CLB2-R336A,R379A,K383A-HYGR, trp1::pGAL-NDD1-9xMYC-TRP1*	[7]
HN01	*clb3Δ::pAgTEF-KANMX-tAgTEF, trp1::pGAL-NDD1-9xMYC-TRP1*	This Study
HN02	*clb1Δ::pAGTEF-NATNT-tADH1, trp1::pGAL-NDD1-9xMYC-TRP1*	This Study
HN03	*clb3Δ::pAgTEF-KANMX-tAgTEF, clb2::CLB2-R336A,R379A,K383A-HYGR, trp1::pGAL-NDD1-9xMYC-TRP1*	This Study
HN04	*clb1Δ::pAGTEF-NATNT-tADH1, clb2::CLB2-R336A,R379A,K383A-HYGR, trp1::pGAL-NDD1-9xMYC-TRP1*	This Study
HN05	*clb3Δ::pAgTEF-KANMX-tAgTEF, clb1Δ::pAGTEF-NATNT-tADH1, trp1::pGAL-NDD1-9xMYC-TRP1*	This Study
HN06	*clb3Δ::pAgTEF-KANMX-tAgTEF, clb1Δ::pAGTEF-NATNT-tADH1, clb2::CLB2-R336A,R379A,K383A-HYGR, trp1::pGAL-NDD1-9xMYC-TRP1*	This Study
DOM1324	*SPC42-mCherry-HIS3*	[60]
HN24	*SPC42-mCherry-HIS3, clb2::CLB2-R336A,R379A,K383A-HYGR*	This Study
DOM1228	*pds1::PDS1-myc13-TRP1*	[61]
HN10	*pds1::PDS1-myc13-TRP1, clb2::CLB2-R336A,R379A,K383A-HYGR*	This Study
HN18	*pds1::PDS1-myc13-TRP1, clb3Δ::pAgTEF-KANMX-tAgTEF*	This Study
HN19	*pds1::PDS1-myc13-TRP1, clb1Δ::pAgTEF-NATNT-tADH1*	This Study
HN13	*pds1::PDS1-myc13-TRP1, clb3Δ::pAgTEF-KANMX-tAgTEF, clb2::CLB2-R336A,R379A,K383A-HYGR*	This Study
HN16	*pds1::PDS1-myc13-TRP1, clb1Δ::pAgTEF-NATNT-tADH1, clb2::CLB2-R336A,R379A,K383A-HYGR*	This Study
HN22	*pds1::PDS1-myc13-TRP1, clb3Δ::pAgTEF-KANMX-tAgTEF, clb1Δ::pAGTEF-NATNT-tADH1*	This Study
HN21	*pds1::PDS1-myc13-TRP1, clb3Δ::pAgTEF-KANMX-tAgTEF, clb1Δ::pAgTEF-NATNT-tADH1, clb2::CLB2-R336A,R379A,K383A-HYGR*	This Study
HN43	*pds1::PDS1-myc13-TRP1, swe1Δ::pAgTEF-NATNT-tADH1*	This Study
HN44	*pds1::PDS1-myc13-TRP1, swe1Δ::pAgTEF-NATNT-tADH1, clb2::CLB2-R336A,R379A,K383A-HYGR*	This Study
DW03	*pds1::PDS1-myc13-TRP1, swe1Δ::pAgTEF-NATNT-tADH1, clb3Δ::pAgTEF-KANMX-tAgTEF, clb1Δ::pAgTEF-NATNT-tADH1*	This Study
DW04	*pds1::PDS1-myc13-TRP1, swe1Δ::pAgTEF-NATNT-tADH1, clb3Δ::pAgTEF-KANMX-tAgTEF, clb1Δ::pAgTEF-NATNT-tADH1, clb2::CLB2-R336A,R379A,K383A-HYGR*	This Study
DOM1231	*pds1::PDS1-MYC-TRP1, mad2Δ::KAN*	[61]
HN39	*pds1::PDS1-MYC-TRP1, mad2Δ::KAN, clb2::CLB2-R336A,R379A,K383A-HYGR*	This Study
DW01	*pds1::PDS1-MYC-TRP1, mad2Δ::KAN, clb3Δ::pAgTEF-KANMX-tAgTEF, clb1Δ::pAgTEF-NATNT-tADH1*	This Study
DW02	*pds1::PDS1-MYC-TRP1, mad2Δ::KAN, clb3Δ::pAgTEF-KANMX-tAgTEF, clb1Δ::pAgTEF-NATNT-tADH1, clb2::CLB2-R336A,R379A,K383A-HYGR*	This Study
HN41	*pds1::PDS1-myc13-TRP1, apc1::APC1Δ225-365-NATNT*	This Study
HN42	*pds1::PDS1-myc13-TRP1, apc1::APC1Δ225-365-NATNT, clb2::CLB2-R336A,R379A,K383A-HYGR*	This Study
HZY292	*ura3–52, leu2Δ1, trp1Δ63, his3Δ200, lys2ΔBgl, arg4Δ, sml1Δ::TRP1, hom3–10, ade2Δ, ade8, ade8 has 2 NT loss, S288c*	[62]
HN07	*ura3–52, leu2Δ1, trp1Δ63, his3Δ200, lys2ΔBgl, arg4Δ, sml1Δ::TRP1, hom3–10, ade2Δ, ade8, ade8 has 2 NT loss, clb2::CLB2-R336A,R379A,K383A-HYGR, S288c*	This Study
DOM77	*sic1Δ::LEU2 + pAB1234-2micron Gal-CLB2-TAP-URA3*	[1]
MO840	*sic1Δ::LEU2 + pAB1234-clb2-2micron Gal-CLB2-R336A,R379A,K383A-TAP-URA3*	[7]

Table S4. Plasmids used in this work.

Name	Description	Source
pEV652	pET11a-Cks1 (untagged)	[20]
pEV653	pET11a-Cks1 mutant (R33A/S82E/R102A)	[8]
pHN37	pET28a-6xHis-SUMO-Fun30 (1-550)	This Study
pHN43	pET28a-6xHis-SUMO-Ssk1 (71-220)	This Study
pHN44	pET28a-6xHis-SUMO-Cdc27 (241-360)	This Study
pHN45	pET28a-6xHis-SUMO-Cdc16 (1-180)	This Study
pHN46	pET28a-6xHis-SUMO-Spa2 (524-670)	This Study
pHN47	pET28a-6xHis-SUMO-Bud6 (126-360)	This Study
pCC84	pLIB-Cdk1 (untagged)	[48]
pCC85	pLIB-6xHis-Myc-Cyclin B1	[48]
	pLIB-His-TEV-Cks1	[49]
pHN31	pET28a-6xHis-GST-TEV-hAPC3 (157-457)	This Study